THE PREPARATION, MULTINUCLEAR MAGNETIC RESONANCE AND SOLID-STATE INVESTIGATION OF SOME CLASSICALLY BONDED ANIONS OF THE HEAVY MAIN-GROUP ELEMENTS DERIVED FROM ZINTL PHASES

THE PREPARATION, MULTINUCLEAR MAGNETIC RESONANCE AND SOLID-STATE INVESTIGATION OF SOME CLASSICALLY BONDED ANIONS OF THE HEAVY MAIN-GROUP ELEMENTS DERIVED FROM ZINTL PHASES

by

LESLEY ANN DEVEREUX B.Sc.

A Thesis

Submitted to the School of Graduate Studies

In Partial Fulfillment of the Requirements

for the Degree

Master of Science

McMaster University

SEPTEMBER, 1985

MASTER OF SCIENCE (1985) McMaster University
Chemistry Hamilton, Ontario

TITLE: The Preparation, Multinuclear Magnetic Resonance and Solid-State Investigation of Some Classically Bonded Anions of the Heavy Main-Group Elements Derived from Zintl Phases.

AUTHOR: Lesley Ann Devereux, B.Sc. (McMaster University)

SUPERVISOR: Dr. G. J. Schrobilgen

NUMBER OF PAGES: 102

ABSTRACT

The synthesis and X-ray crystallographic determination of solid derivatives of homo- and heteropolyatomic anions derived from Zintl phases has generally yielded the least soluble of the ions present in solution. Many other species present in these solutions have remained unidentified until recently when considerable effort directed towards the investigation of the solution chemistries of Zintl anions has been put forth.

The present work is mainly concerned with the characterization of new Zintl anions in solution using multinuclear magnetic resonance spectroscopy as the primary investigative tool. These studies include (1) the tetrahedral $SnCh_4^{4-}$ (Ch = selenium and/or tellurium), (2) the dimer of $SnSe_3^{2-}$, $Sn_2Se_6^{4-}$, (3) several interesting but, as-of-yet, unidentified species present in solutions derived from ternary Na/Sn/Te alloys and present in the reaction of Sn(II) Cl_2 with Te_2^{2-}, and (4) a set of possible multi-thallium-tellurium species. Relevant chemical shifts and nuclear spin-spin coupling constants are reported and trends discussed.

^{119}Sn Mössbauer investigations of all tin-containing species is also presented as is a brief discussion of the X-ray crystallographically determined polytelluride, Te_4^{2-}.

ACKNOWLEDGEMENTS

I would like to take this opportunity to express my appreciation to those who have contributed so much to this project.

To Drs. A. Bain and C. A. Rodger of Bruker Spectrospin Canada for their time, equipment and expertise in obtaining the thallium NMR spectra.

To Dr. T. Birchall for obtaining the ^{119}Sn Mössbauer data.

To my co-worker Mar Björgivinsson for all his valuable help and many interesting discussions.

To Dr. G. J. Schrobilgen for all his help especially in the preparation of this thesis.

To Dr. R. C. Burns for providing the ideas for this project and without whose help and guidance this project could not have been done.

To Carol Dada for typing this thesis and withstanding my constant harassment.

To Toad Syvret for his help in getting me through these last two years, his constant encouragement and his friendship.

To McMaster University and the Department of Chemistry for providing my scholarship and the opportunity to do this work.

To all my friends for making my years at McMaster the best years of my life.

TABLE OF CONTENTS

LIST OF TABLES

LIST OF FIGURES

LIST OF FIGURES (Continued)

CHAPTER I

INTRODUCTION

Synthetic and Structural Background

In recent years, renewed interest in the chemistry of the main group elements has provided a wealth of novel inorganic compounds. The condensation of inorganic chains to rings and polymeric networks[1,2] represents a small fraction of the current work in this field. An area of great interest concerns the study of clusters, rings and cages of the heavier B subgroup i.e., Pb, Sn and Bi.[2,3] Many of the heavy main group elements are known to form intermetallic phases (Zintl phases) with alkali metals which give soluble products in liquid NH_3 or ethylene-diamine (en).

Although the first examples of the species now designated "Zintl ions" were reported by Johannis[4] in 1891, it was not until about 50 years ago that Zintl and co-workers[5-7] described their electrochemical studies on solutions of such sodium alloys. The homopolyatomic anions Sn_9^{4-}, Pb_9^{4-}, Bi_7^{3-}, Sb_7^{3-} and Te_4^{2-} were among the first species to be identified. Attempts made to isolate the salts of these anionic species by evaporation of the solvent led only to the formation of amorphous products or reversion to a known binary alloy phase(s), e.g.

$$(Na(NH_3)_n^+)_3Sb_7^{3-} \xrightarrow{evap.} 3NaSb(s) + 4Sb + 3nNH_3(g) \qquad (1)$$

Such decomposition naturally prevented any structural studies from taking place on these homopolyatomic anions.

More recently, Kummer and Diehl[8] were able to isolate the first salt of a Zintl species using ethylenediamine (en) as their solvent in the compound $Na_4Sn_9 \cdot 7(en)$. The compounds $Na_4Ge_9 \cdot 5(en)$ and $Na_3Sb_7 \cdot 4(en)$ were also isolated and identified by elemental analyses.[9,10] Furthermore, an incomplete crystal structure of the tin compound[9,10] revealed a distorted and disordered Sn_9^{4-} anion.

It was through the use of a macrobicyclic ligand 2,2,2-crypt (Fig. 1a), hereafter designated "crypt",[11,12] that the isolation of many Zintl anions was realized. The macrocycle successfully complexed the alkali metal counterion (Na^+ or K^+) in solution preventing the formation of other more stable intermetallic phases upon solvent removal. The solubility of the Zintl salts in the ammonia and particularly the amine solvents, is also increased by the presence of crypt. The crypt ligand contains a three-dimensional intramolecular cavity which strongly binds the alkali metal ion, forming stable inclusion complexes (Fig. 1b).[13] Corbett and co-workers[14-21] have used this complexing ability of crypt to isolate and stabilize a variety of homopolyatomic anions, characterized by X-ray crystallography and summarized in Table 1.

As can be seen in Table 1, these clusters have many isoelectronic and sometimes isostructural analogs found among the main group homopolyatomic cations and, of course, the

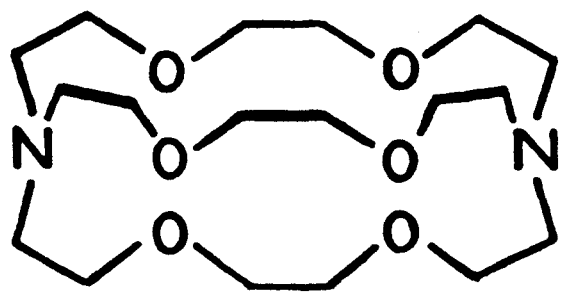

Fig. 1a). 4,7,13,16,21,24-hexaoxa-1,10-diazobicyclo[8.8.8] hexacosane; 2,2,2-crypt.

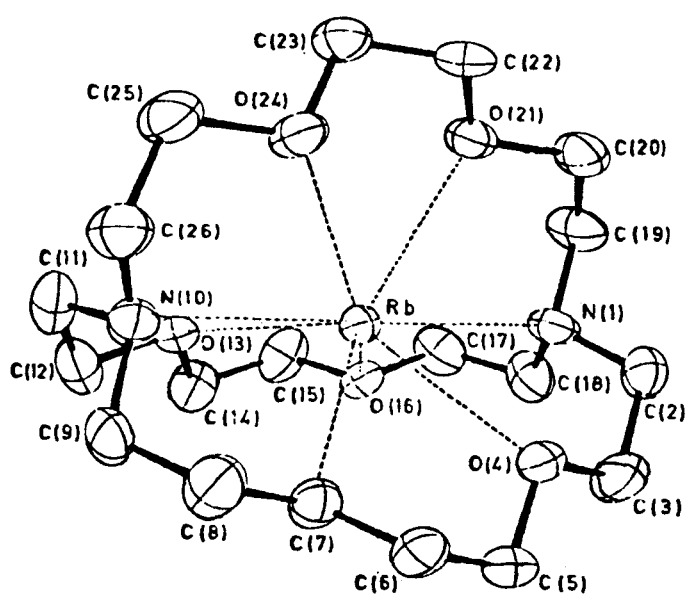

Fig. 1b). Structure of a Rubidium "Cryptate". (13)

TABLE I

HOMOPOLYATOMIC ANIONS OF KNOWN STRUCTURE[a]

Anion	Symmetry	Isoelectronic Analogs	Str. Ref.
Ge_9^{2-}	$C_{2v}(\sim D_{3h})$	$B_9H_9^{2-}$	14
Ge_9^{4-}	C_{4v}	$Bi_9^{5+}(D_{3h})$	14
Sn_9^{4-}	C_{4v}	$Bi_9^{5+}(D_{3h})$	15
Sn_9^{3-}	D_{3h}	-	16
Sn_5^{2-} Pb_5^{2-}	D_{3h}	Bi_5^{3+}	17
Sb_4^{2-}	D_{4h}	Te_4^{2+}, Se_4^{2+}	18
Bi_4^{2-}			19
As_{11}^{3-}	$\sim D_3$	P_{11}^{3-}	20
Sb_7^{3-}	C_{3v}	As_7^{3}, P_7^{3-}	18,21

[a] Crypt-K^+ or Crypt-Na^+ salts.

boranes ($B_nH_n^{2-}$). The structures of all of the polyanions can be predicted on the basis of Wade's rules[22,23] if one assumes that each metal atom in a potential polyatomic cluster has an exo-skeletal electron lone-pair which is not involved in the bonding. Corbett[24] has noted that a range of 2-3 p-electrons per element is necessary for cage and cluster species to exist. This electronic complement is found in those anions listed in Table 1, e.g. both Sn_5^{2-} and Pb_5^{2-} contain 22 valence electrons, have formal skeletal electron counts of 2n+2 and possess trigonal bipyramidal structures (D_{3h}) analogous to the closo-$B_5H_5^{2-}$ anion. It should also be noted that no evidence for homopolyanions of the elements to the left of group IV exists. This is because in order to satisfy the minimum electronic requirements, electro-positive elements such as mercury and thallium would require very high and energetically unfavourable anionic charges to be associated with each element.[25]

Mixed metal systems in which elements like mercury and thallium, with their relatively low numbers of valence electrons, are combined with less electro-positive, more electron-rich elements has led to the stabilization and characterization of heteropolyatomic species such as $Tl_2Te_2^{2-}$,[25] $TlSn_8^{3-}$,[26] $TlSn_9^{3-}$,[26] and $HgTe_2^{2-}$,[27]. Again, through the application of Wade's rules, the geometries of species such as $TlSn_9^{3-}$ and $Tl_2Te_2^{2-}$ can be rationalized. The $Tl_2Te_2^{2-}$ anion contains 2n+4=12 skeletal electrons(n=4), and can be said to be derived from a pentagonal bipyramid, with the capping atomic position

vacant and the geometry distorted to form the open butterfly-shaped anion seen in Fig. 2C.

The $HgTe_2^{2-}$ anion was found to be a classical, linear centro-symmetric anion, and is one of only a few examples in which the bonding of a polyatomic anion is deemed to be strictly classical. The $SnTe_4^{4-}$,[28] and $SnSe_4^{4-}$,[29] anions are essentially electron-rich, therefore possess classically-bonded, tetrahedral structures with an octet of electrons surrounding the central tin atom. Heteropolyatomic electron-rich anions also isolated include the tetrahedral $Sn_2Bi_2^{2-}$,[30] and $Pb_2Sb_2^{2-}$,[31] species (Fig. 2).

Early Solution Studies

The late R. W. Rudolph and his co-workers[32-35] have provided a significant portion of the information available regarding solution studies of Zintl anions through the use of multinuclear magnetic resonance spectroscopy. Alloys of the following compositions, $Na_{1\rightarrow2}Sn$, $NaSn_{2.25}$, NaSnPb, NaSnGe, KSnGe and $NaSnTl_{1.5}$, were extracted in en and liquid NH_3 in the absence of crypt. The homopolyatomic anions Sn_4^{2-}, Sn_9^{4-}, Pb_9^{4-} and the mixed-metal anions $Sn_{9-n}Pb_n^{4-}$ (n=1-8), $Sn_{9-n}Ge_n^{4-}$ (n=1-8) and $TlSn_8^{5-}$ have been characterized by ^{119}Sn and ^{207}Pb NMR spectroscopy.[32-35]

In the case of the Sn_9^{4-} cluster, the single ^{119}Sn resonance observed was split, due to ^{119}Sn-^{117}Sn spin-spin coupling, into a multiplet whose intensity distribution corres-

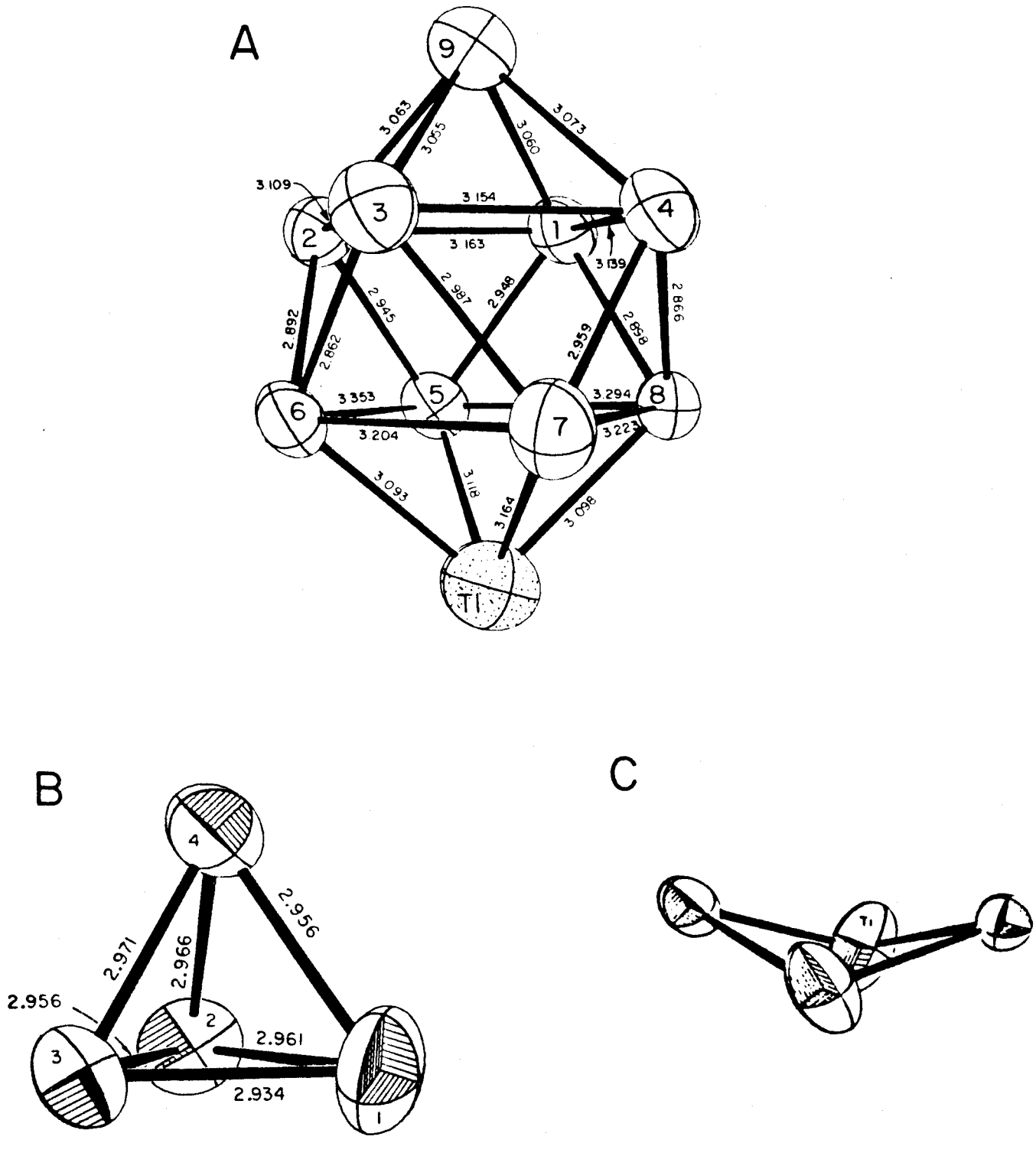

Fig. 2. Structures of Some Heteropolyatomic Zintl Anions. (A) The $TlSn_9^{3-}$ anion in $(2,2,2\text{-crypt-}K^+)_6(TlSn_9^{3-}TlSn_8^{3-})\cdot 2en$ (26); (B) Disordered $Sn_2Bi_2^{2-}$ anion $(2,2,2\text{-crypt-}K^+)_2Sn_2Bi_2^{2-}$ (30); (C) The $Tl_2Te_2^{2-}$ anion in $(2,2,2\text{-crypt-}K^+)_2Tl_2Te_2^{2-}\cdot en$ (25).

ponded to that calculated for a nine-atom polyhedron.[32,33] More importantly, the observation of only a single ^{119}Sn resonance unequivocally established that the three tin environments associated with the monocapped square-antiprismatic geometry of Sn_9^{4-}, were undergoing a rapid INTRAMOLECULAR exchange on the NMR time scale. The fluxionality of Sn_9^{4-} had been predicted[15] and, in fact, all of the nine-atom polyanions have been found to be fluxional in nature. This invaluble work clearly established the importance of multinuclear magnetic resonance spectroscopy as a complementary structural tool to X-ray crystallography in the study of these systems.

Multinuclear Magnetic Resonance as an Investigative Tool

As part of an ongoing research effort in our laboratory, we have sought to extend the range of known classically-bonded heteropolyatomic anions of the immediate post-transition and main-group elements, using multinuclear magnetic resonance spectroscopy as the primary investigative tool.[36] This approach was a viable one because all of the post-transition elements forming a Zintl phase possess at least one natural abundance isotope which is NMR active (Table 2). Furthermore, many of these elements possess naturally occurring isotopes which are spin-$\frac{1}{2}$ nuclei and, as such, can provide structural information regarding these species based upon their hetero- and homonuclear spin-spin couplings.[33,37]

TABLE 2: Nuclear Properties of NMR Nuclei Studies in this Work[37]

ISOTOPE[a]	NATURAL ABUNDANCE %N	MAGNETOGYRIC RATIO $/10^7 radT^{-1}s^{-1}$	NMR FREQUENCY Ξ/MHz[b]	STANDARD	RECEPTIVITY D[c]
^{77}Se	7.58	5.101	19.091523	$(CH_3)_2Se$	2.98
^{117}Sn	7.61	-9.530	35.632 [c]	$(CH_3)_4Sn$	19.54
^{119}Sn	8.58	-9.971	37.290662	$(CH_3)_4Sn$	25.20
^{123}Te	0.87	-7.011	26.169 [c]	$(CH_3)_2Te$	0.89
^{125}Te	6.99	-8.453	31.549802	$(CH_3)_2Te$	12.50
^{203}Tl	29.50	15.288	-	0.1M thallous acetate in H_2O	$2.89x10^2$
^{205}Tl	70.50	15.438	-		$7.69x10^2$

[a] All nuclei in the above table possess a nuclear spin, I, of I = ½.

[b] The exact frequency is for the standard substance referred to in the above Table, referenced to the protons in TMS which are taken to resonate at precisely 100 MHz.

[c] NMR frequencies obtained from the Handbook of High Resolution Multinuclear NMR.[38]

Our initial solution studies led to the identification of at least four series of classically-bonded anions. These are (1) the linear $HgSe_{2-n}Te_n^{2-}$ anions, (2) the cyclic $Tl_2Se_{2-n}Te_n^{2-}$ anions, (c) the trigonal-planar $TlSe_{3-n}Te_n^{3-}$ and $SnSe_{3-n}Te_n^{2-}$ anions, and (4) the tetrahedral $SnTe_4^{4-}$ and $SnSe_4^{4-}$ anions.[36] The formal oxidation state of the tin series of anions was established by ^{119}Sn Mössbauer spectroscopy.[52] Identification of these Zintl anions was based solely upon correct NMR assignments. The reliability of the assignments was assured by a combination of two or more of the following criteria:

(1) observation of distinct heteronuclear spin-spin coupling patterns resulting from isotopically dilute spin-$\frac{1}{2}$ nuclides;

(2) ^{77}Se or ^{125}Te isotopic enrichment to give the appropriate spin multiplicities corresponding to the number of chalcogenide ligands directly bonded to the nuclide being observed;

(3) identification and consistent behaviour of peaks from the same species in the spectra of two or more of its nuclei. For example, observation of a single peak flanked by a satellite doublet in the ^{119}Sn NMR spectrum of $SnTe_3^{2-}$ yields a value for $^1J_{^{119}Sn-^{125}Te}$; upon finding a

peak in the ^{125}Te NMR spectrum with corresponding $^{117,119}Sn$ satellites, and the same J-value, positive identification of that species is made;

(4) systematic variation of peak intensities as the ratio of tellurium to selenium is changed.

As previously mentioned, Rudolph's[32,33] solution NMR studies proved the fluxionality of the nine-atom polyanions which could not have been ascertained by solid-state methods. Corbett's[25] extraction of the alloy composition KTlTe in en with crypt led only to the identification of the butterfly-shaped $Tl_2Te_2^{2-}$ anion when, in fact, a new series of trigonal-planar thallium species, $TlSe_{3-n}Te_n^{3-}$, was observed in solution along with the mixed cycles $Tl_2Se_{2-n}Te_n^{2-}$.[36]

The value of isotopic enrichment in the elucidation of structural information was elegantly displayed in the study of the $TlCh_3^{3-}$(Ch=Te/Se) anions.[36] The number of signals present and the relative intensities of the multiplet peaks in the ^{205}Tl spectra established the overall $TlCh_3^{3-}$ stoichiometry. However, upon enrichment with 77.3% ^{125}Te, the multiplicity patterns observed in the ^{205}Tl spectra (Fig. 3) for $TlTe_3^{3-}$, $TlTe_2Se^{3-}$ and $TlTeSe_2^{3-}$ were identical to those calculated based upon ^{125}Te abundance and statistical distributions of selenium and tellurium ligand atoms for the assumed trigonal planar structures. An example of the origin of such patterns

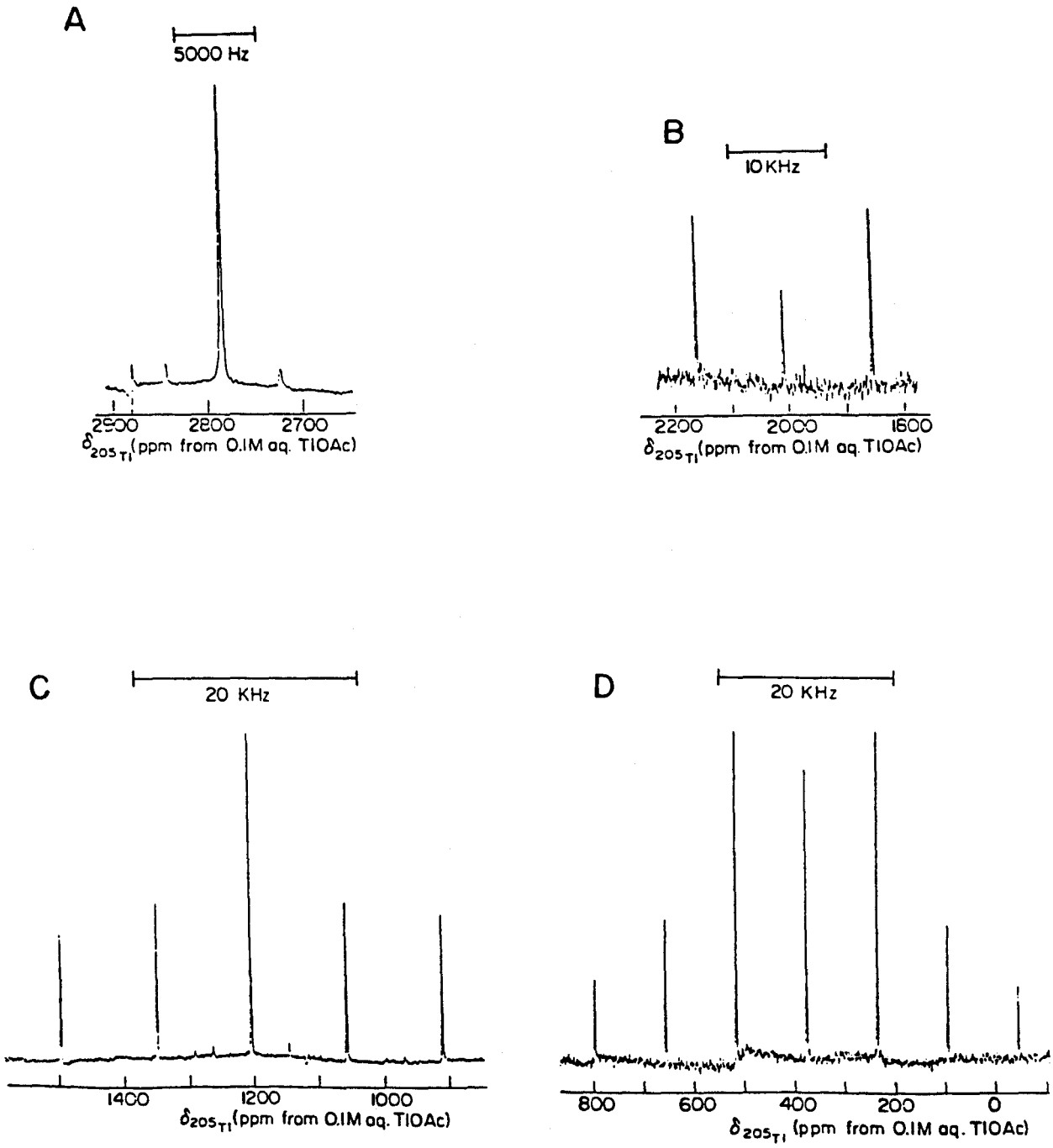

Fig. 3. ^{205}Tl NMR spectra obtained at 57.76 MHz, for the $TlCh_3^{2-}$ series of anions, containing ^{125}Te enriched to 77.3%. The multiplet patterns are assigned as follows: (A) $TlSe_3^{3-}$; (B) $TlSe_2Te^{3-}$; (C) $TlSeTe_2^{3-}$; (D) $TlTe_3^{3-}$.

is given diagramatically in Appendix A-1, along with a listing of the relative intensities for the remaining members in the series.

Structural information deduced from NMR studies is, of course, not limited to those nuclides having a high natural abundance or a high degree of enrichment. For spin-½ nuclei of low abundance, as found in the $SnCh_3^{2-}$ series of anions, (e.g. $^{119}Sn(8.58\%)$, $^{117}Sn(7.61\%)$, $^{125}Te(6.99\%)$ and $^{77}Se(7.58\%)$ etc.) a single, intense resonance was observed, flanked by a satellite doublet or sets of satellite doublets whose separation was exactly the value of the spin-spin coupling constant(s) between two of the nuclei present. A comparison of the satellite intensities relative to the central peak yields the number of equivalent nuclei that each observed environment is coupled to. Appendix A-2 provides sample calculations and satellite intensities for the $SnCh_3^{2-}$ series of anions.

Spin-spin coupling constants can also give valuable information regarding the bonding (hybridization) present in a molecule. Similar J-values indicate similar bonding and affords comparisons to be made between members of isostructural series.

Purpose and Scope of Present Work

The current body of work is basically an extension of the philosophy and chemistry described in the previous section. The behaviour of the ternary and quaternary Zintl phases (i.e. phase diagrams) used during these studies are generally unknown.

In light of this fact, extraction of the alloys in en or liquid NH_3 can give rise to a mixture of phases and correspondingly complex solution chemistries.[36] This is made readily apparent by the presence of polychalcogenide anions in some of the previously described solutions containing classically-bonded tin and thallium species. Current investigations by M. Björgvinsson and G. J. Schrobilgen are under way in the hope of understanding the roles these selenium and tellurium polyanions play in the chemistry of the classically-bonded anions. Previously unidentified resonances found in the NMR spectra of the aforementioned systems have resulted in considerable effort being put forth to assign these species. To this end, extraction of new alloys have in turn led to the observation of other new classically-bonded species in solution. On the surface, it might seem that this work has muddied the simpler picture we had in mind at the start of this project, however it is hoped that the current efforts will ultimately provide some clues leading to a fuller overall understanding of these polyanions and their solution chemistries.

CHAPTER II

EXPERIMENTAL

General

The majority of compounds used and prepared during this work were air and moisture sensitive. Consequently, all manipulations were carried out under anhydrous conditions on glass vacuum lines or in a nitrogen atmosphere drybox (Vacuum Atmospheres Model DLX). Drybox moisture and oxygen levels were routinely less than 0.1 ppm. All apparatus were thoroughly dried by pumping overnight on a vacuum line and were flamed several times with a Bunsen burner while under "hard" vacuum (less than 10^{-4} torr). All weighings of dry air-sensitive substances were performed inside the drybox.

Potassium and Sodium

Potassium (MCB) and sodium (BDH Chemicals, 99.8%) required cleaning and drying before use. Large pieces of potassium (or sodium) were thoroughly rinsed in petroleum ether to remove the paraffin oil coating and the outer layers were cut off to expose a fresh metal surface. The metal was then quickly sliced into smaller pieces and immediately transferred to a glass storage vessel which was evacuated and placed in a drybox for storage until used.

Anhydrous $Sn(II)Cl_2$

$SnCl_2 \cdot 2H_2O$ (Baker Analyzed, 98.6%) was dehydrated with acetic anhydride (Fischer Scientific Co.), filtered, and washed with anhydrous ether (Fischer Scientific Co.). The product was placed in a glass storage vessel, pumped out overnight and stored in a drybox.

Solvents

Ethylenediamine (Fischer Scientific Co.) was dried over CaH_2 (MCB) for several weeks and then vacuum distilled onto and stored over fresh CaH_2 for at least one week prior to use.

Ammonia (Canadian Liquid Air) was condensed from a cylinder into a large tube connected to a vacuum line and containing sodium metal for drying purposes. The liquid ammonia was stored over sodium at -78°C for at least one week before use.

Reaction of $SnCl_2$ and Te_2^{2-}

K_2Te (provided by Már Björgivinsson) and a stoichiometric amount of tellurium powder were placed in one arm of a two-armed reaction vessel and the corresponding desired amount of $SnCl_2$ was placed in the other arm of the reaction vessel. Approximately 10 cm^3 of en was statically distilled onto the K_2Te/Te powder mixture at 0°C. After warming the solution to room temperature, a blue-violet color was observed and deepened as the reaction proceeded. The reaction was allowed to continue for about 1 week then the intense blue-violet solution (Te_2^{2-}) was decanted over onto the $SnCl_2$ in the other arm of

the reaction vessel.

Alloy Preparation

Tin (Baker Analyzed, 99.9%), thallium (BDH, 99.999%), tellurium (Alfa Inorganics, 99.5%) and selenium (Alfa Inorganics, 99.9%) were used directly as obtained while the potassium and sodium metals were prepared as previously described and re-trimmed to reveal clean metal surfaces just prior to use in the atmosphere of the drybox. Approximately 1.0 g of freshly cut alkali metal was used for each alloy preparation. All alloys were prepared by fusion of the alkali metal with either tin or thallium to give a binary alloy ($\sim$ 1:1 mole ratio) in thick-walled Pyrex fusion vessels using a Meeker burner. The required amounts of selenium and/or tellurium were pre-mixed, added to the binary alloy in the drybox and the mixture heated gently until the metals reacted. After the initial violent reaction had subsided, the resulting alloy was kept in a molten state and mixed thoroughly to ensure homogeneity. After complete reaction the vessel was allowed to cool and then transferred into a drybox where the glass vessel was broken apart. The alloy was then collected, powdered and stored in a glass vial until required. In almost every case involving sodium-tin alloys, a plug of tin metal was recovered from the final alloy (typically 20-30% of the initial mass of tin added) so that the sodium-tin alloys contain somewhat less than the indicated amount of tin. Table 3 lists all the alloys prepared during this work with their corrected

TABLE 3: Composition of the Alloys Prepared

Alloy	Elemental Composition (x 10^{-2} mole)					
	K	Na	Sn[a]	Tl	Se	Se
$NaTlTe_2$		2.794		2.797		5.587
NaTlTeSe		3.706		3.706	3.714	3.710
$NaTlTe_{1.5}Se_{0.5}$		2.183		2.181	1.092	3.274
$NaTlSe_2$		1.983		1.984	4.148	
$KSnSe_2$	2.308		2.308		4.617	
$KSnTe_2$	1.956		1.956			3.912
NaSnTe		4.841	4.838 (3.452)			4.839
NaSnSe		4.417	4.418 (3.534)		4.417	
$NaSnTe_{0.67}Se_{0.33}$		3.839	3.839 (2.879)		1.279	2.559
$NaSnTe_{0.33}Se_{0.67}$		3.738	3.738 (3.177)		2.492	1.246
$NaSn_2Te_{1.5}$		4.172	8.354			6.261
$NaSn_{1.5}Te$		2.727	4.099			2.732

[a] Values in parentheses represent tin compositions after the amount of unreacted tin has been corrected for.

compositions where applicable.

Extraction of the Alloy Phases

2,2,2-crypt (4,7,13,16,21,24-hexaoxa-1,10-diazobicyclo [8.8.8] hexacosane) (Merck) was used as received. Approximately 150-200 mgs of the powdered alloys were mixed with a 2-5 mole percent excess of crypt in a drybox. This mixture was then transferred to an evacuated glass reaction vessel (Fig. 4), re-evacuated and typically 10 cm^3 of en (or $NH_3(\ell)$) statically distilled onto the alloy/crypt mixture. Immediate reaction producing intensely colored solutions was observed. Complete reaction of the alloys generally took place within five to ten days and the samples were agitated several times daily during the extraction period.

Preparation of NMR Samples

Following extraction of the alloy phases, the solid residues were allowed to settle and then the clear, colored solutions were decanted into precision 10 mm (o.d.) (thick-walled for $NH_3(\ell)$ NMR tubes attached to the reaction vessels (Fig. 4). The solutions were concentrated for NMR analysis through evaporation by cooling the portion of the reaction vessel containing the residual alloy in ice-water. Slow static distillation of en or $NH_3(\ell)$ from the NMR tube back onto the alloy was allowed to continue until a solvent column height suitable for NMR analysis was obtained or until a saturated solution had formed. If the solid residue dissolved

Fig. 4 Reaction Vessel for Alloy Extraction

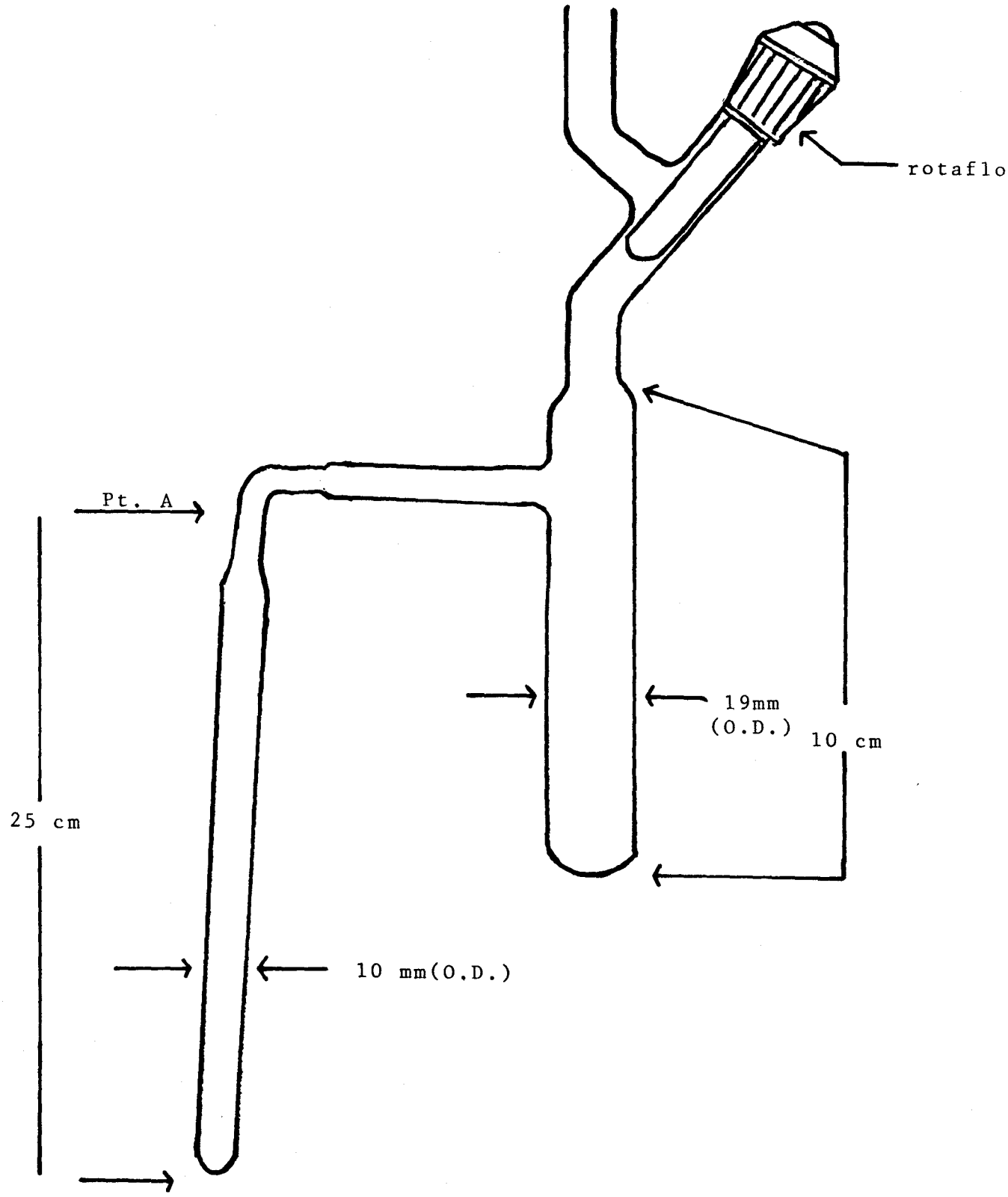

producing a colored solution, the concentration process was repeated until the solvent over the residue was colorless. After cooling the NMR tube and the reaction arm to 0°C in the case of en or -78°C for $NH_3(\ell)$, the NMR tube and contents were isolated by flame sealing at point A in Fig. 4.

In general, concentrations of the anions ranged from about 0.05 molal to 0.25 molal. The approximate distributions of the anions extracted from the quaternary alloys were estimated from relative NMR signal intensities and are as follows:

$NaSnTe_{0.67}Se_{0.33}$ - 19% $SnTe_4^{4-}$, 38% $SnTe_3Se^{4-}$, 31% $SnTe_2Se_2^{4-}$, 12% $SnTeSe_3^{4-}$, < 1% $SnSe_4^{4-}$;

$NaSnTe_{0.33}Se_{0.67}$ - < 1% $SnTe_4^{4-}$, 3% $SnTe_3Se^{4-}$, 19% $SnTe_2Se_2^{4-}$, 43% $SnTeSe_3^{4-}$, 35% $SnSe_4^{4-}$

Multinuclear Magnetic Resonance Spectroscopy

All NMR spectra were recorded on pulse spectrometers equipped with cryomagnets and consequently were run unlocked (field drift < 0.1 Hz/m). The observing frequencies were ^{77}Se (47.70 MHz), ^{119}Sn (93.273 MHz), and ^{125}Te (78.917 MHz) when spectra were recorded at an external applied field strength of 5.8719 Tesla on a Bruker WM-250 spectrometer using 10 mm probes which were broad-banded over the frequency ranges 23 to 103 MHz.

When spectra were recorded at an external applied field strength of 7.0463 T on a Bruker AM-300 spectrometer the observing frequencies were ^{125}Te (94.692 MHz) and ^{119}Sn (111.922 MHz). Free induction decays were typically accumulated in a 32 K memory, spectral width settings of 25 to 100 KHz were employed yielding data point resolutions of 1.5 to 6.1 Hz and acquisition times of 0.164 to 0.655 s, respectively. No relaxation delay was applied. The number of free induction decays accumulated varied with concentration and sensitivity of the nucleus under consideration, with 10,000 to 300,000 scans being typical for these dilute samples. Pulse widths corresponding to bulk magnetization tip angles, θ, of approximately 90° were 20(^{77}Se), 25(^{125}Te) and 10μs(^{119}Sn). Line broadening parameters used in exponential multiplication of the free induction decays were 10 to 20 Hz.

Because ^{203}Tl and ^{205}Tl resonate outside the dynamic range of the Bruker WM-250 high-range probe (142.87 and 144.27 MHz, respectively, at 5.8719 Tesla), the NMR spectra of these nuclei were obtained on a Bruker WP-100 SY/SC (Bruker Canada Applications Laboratory, Milton, Ontario) at an applied field of 2.3488 Tesla. This was achieved by using a 10 mm broad-band probe from a Bruker WM-360, which tuned over the range 16 to 146 MHz, and which physically fit the WP-100 cryomagnet. The observing frequencies were 57.199 (^{203}Tl) and 57.760 MHz (^{205}Tl) with pulse widths of 10 μs (θ = 90°).

The respective nuclei were referenced to neat samples of $(CH_3)_2Se$, $(CH_3)_2Te$, $(CH_3)_4Sn$ and to a 0.1 M aqueous TlOAc solution at 24°C. The chemical shift convention used is a positive sign signifies a chemical shift to high frequency of the reference compound and vice-versa.

Preparation of Tin Mössbauer Samples

The required amount of alloy (∿ 60 mg) was extracted according to the procedures outlined in previous sections of this work. The extract solution, however, was evaporated to dryness on a glass vacuum line and the tube and contents heat sealed under vacuum. The sample was transferred to a drybox, cut open and the crypt-salt ground to a fine powder. This powder was placed in a previously dried Kel-F planchette and packed tightly to make an even layer of material (Fig. 5). Teflon spacers were added in order to prevent any slippage of material during analysis if the available material was not sufficient to completely fill the sample holder. The top of the planchette was screwed down tightly on top of the powdered material and the sample was placed in liquid N_2 for storage. In the case of frozen solution samples, the solution was syringed into the Kel-F holder in a glove bag purged constantly with dry N_2. The sample was then placed in liquid N_2 and the ^{119}Sn Mössbauer spectrum obtained.

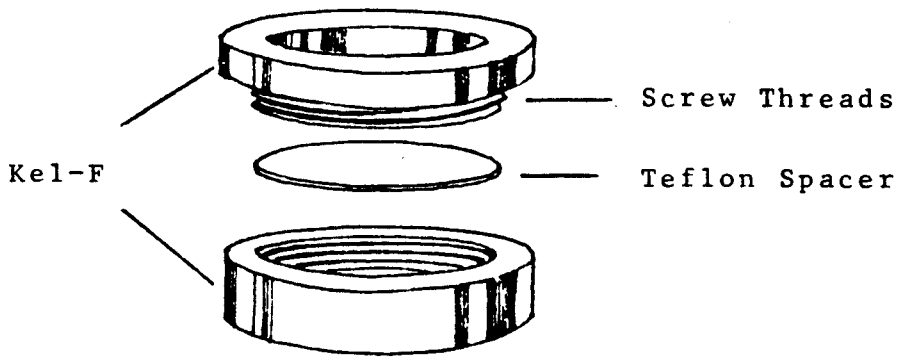

Fig. 5: Sample Holder Used During Mössbauer Experiments

^{119}Sn Mössbauer Spectroscopy

Mössbauer spectra were recorded using an Elscint AME 40 drive system operating in the constant acceleration mode with automatic folding of the triangular waveform. The transmitted radiation, through a Pd filter, was detected by a NaI scintillation counter and fed to a Promeda multi-channel analyzer operating in the up-down multi-scaling mode.[38] Samples were rigidly held in a Liquid Transfer Cryotip system manufactured by Air Products and Chemicals Inc. The source was $Ca^{119m}SnO_3$ purchased from Amersham-Searle and was maintained at room temperature throughout while the samples were cooled to low temperature. The apparatus was periodically calibrated with use of ^{57}Co/Rh and a standard iron foil. Spectra were computer fitted using the program of Stone, which has been modified by Dr. D. Grundy of the McMaster University Geology Department.[39]

[Na-crypt]$_2$[Te$_4$] Crystal Growth and Structure Determination

The $NaTlTe_2$ alloy was prepared and extracted in the presence of crypt in a two-arm reaction vessel, as previously described. The alloy/crypt/en mixture was allowed to stand for two weeks, during which time crystalline material was observed coming out of solution. The solution was warmed to 50°C, all of the solid material re-dissolved and the resulting solution decanted over into the other arm of the reaction vessel leaving the unextracted alloy residue behind. The two-arm

vessel was then placed slightly tilted, in a large dewar filled with hot (50°C) water. The water bath was allowed to cool to room temperature over a period of 72 hours while large crystals were deposited along the sides of the tube. The crystals were isolated by decantation of the supernatant liquid back over onto the alloy residue and the arm of the vessel containing the crystals only, was heat sealed. The crystals were then vacuum dried, placed in a drybox equipped with a microscope, cleaved into smaller fragments and sealed in 0.3 mm Lindemann capillaries. The structure was solved by Dr. J. F. Sawyer using conventional heavy atom techniques (see reference 66 for details).

CHAPTER III

PREPARATION AND NMR SPECTROSCOPIC STUDIES OF THE $SnCh_4^{4-}$ ANIONS (Ch= Te AND/OR Se)

INTRODUCTION

In view of the fact that Rudolph and co-workers[33] had observed the ^{119}Sn and ^{125}Te spectra of $SnTe_4^{4-}$ and the crystal structures of Na_4SnTe_4 and $Na_4SnSe_4 \cdot 16H_2O$ have recently been reported,[28,29] two tin-containing quaternary alloys were prepared, one tellurium rich, the other selenium rich, with the view in mind to observe the tetrahedral $SnSe_{4-n}Te_n^{4-}$ (n=0-4) series of anions. However, alloys of composition $KSnTe_{0.5}Se_{1.5}$ and $KSnTe_{1.5}Se_{0.5}$ yielded solutions containing the trigonal-planar, $SnCh_3^{2-}$, series of anions[36] with no apparent NMR evidence for the presence of even low concentrations of any of the previously characterized tin species, i.e., Sn_9^{4-}, $SnTe_4^{4-}$ or $SnSe_4^{4-}$.

RESULTS AND DISCUSSION

Anions Extracted from $NaSnTe_{1-x}Se_x$ (x=0, 1/3, 2/3, 1) Alloys

Extractions of the ternary alloys NaSnTe and NaSnSe with en in the presence of crypt yielded solutions containing single intense NMR peaks in the ^{119}Sn NMR spectra at -1823.6

ppm and -476.6 ppm from $(CH_3)_4Sn$, flanked by ^{125}Te and ^{77}Se satellite doublets, respectively. The ratios of the heights of the satellite peak to the central peak showed that each tin environment was bonded to four chemically and magnetically equivalent tellurium or selenium atoms. Observation of the ^{125}Te and ^{77}Se NMR spectra allowed the magnitudes of the satellite spacings, and therefore the nuclear spin-spin coupling constants, to be compared in each spectrum and correctly assigned as $^{1}J_{^{119}Sn-^{125}Te}$ = 2851 Hz and $^{1}J_{^{119}Sn-^{77}Se}$ = 1463 Hz. The ^{119}Sn chemical shift and coupling constant for the most shielded resonance agree with those values reported by Rudolph and co-workers[33] for the $SnTe_4^{4-}$ anion, and as such were assigned to $SnTe_4^{4-}$. Similarly, the remaining signal was assigned to the analogous $SnSe_4^{4-}$ anion and both anions are assumed to possess tetrahedral geometries as found for the solid-state structures of these species.[28,29] However, the ^{125}Te chemical shift quoted by Rudolph (-604.4 ppm) differs by a significant amount ($\sim$ 400 ppm) from the value observed in this work (-212.4 ppm). It is believed that the value for the ^{125}Te chemical shift reported in the present work is the correct value after a careful examination of the acquisition parameters was made and no inconsistencies in the present data were found. One can only conclude that there is, in fact, a referencing problem of some sort associated with Rudolph's result.

Extraction of the quaternary alloys $NaSnTe_{0.67}Se_{0.33}$ and $NaSnTe_{0.33}Se_{0.67}$ under the same conditions as above resulted in cherry-red and orange-red colored solutions. A total of five ^{119}Sn NMR signals were found in the solutions extracted from these mixtures. The most shielded resonance is due to $SnTe_4^{4-}$ and the most deshielded is due to $SnSe_4^{4-}$. Both ^{77}Se (Fig. 6) and ^{125}Te NMR spectra showed four lines one each due to the corresponding parent anion $SnCh_4^{4-}$ (Ch=Te or Se) in the tetrahedral series of anions $SnSe_{4-n}Te_n^{4-}$ (n=0-4) and the three remaining signals due to the mixed species. Assignment of these NMR signals was possible, in every case, by observation of the natural abundance satellite doublets resulting from directly-bonded spin-spin coupling between the spin-$\frac{1}{2}$ nuclei ^{119}Sn-^{125}Te, ^{117}Sn-^{125}Te, ^{119}Sn-^{77}Se and ^{117}Sn-^{77}Se. The observation of natural abundance satellite spectra enabled unambiguous assignments to be made for the remaining members of the series based on the following considerations:

1. $^{117,119}Sn$-^{125}Te spin-spin couplings are always larger in an homologous series than the corresponding $^{117,119}Sn$-^{77}Se spin-spin couplings by virtue of the larger magnetogyric ratio of ^{125}Te relative to that of ^{77}Se [37]
2. the spin-spin couplings could be observed in the spectra of each pair of coupled

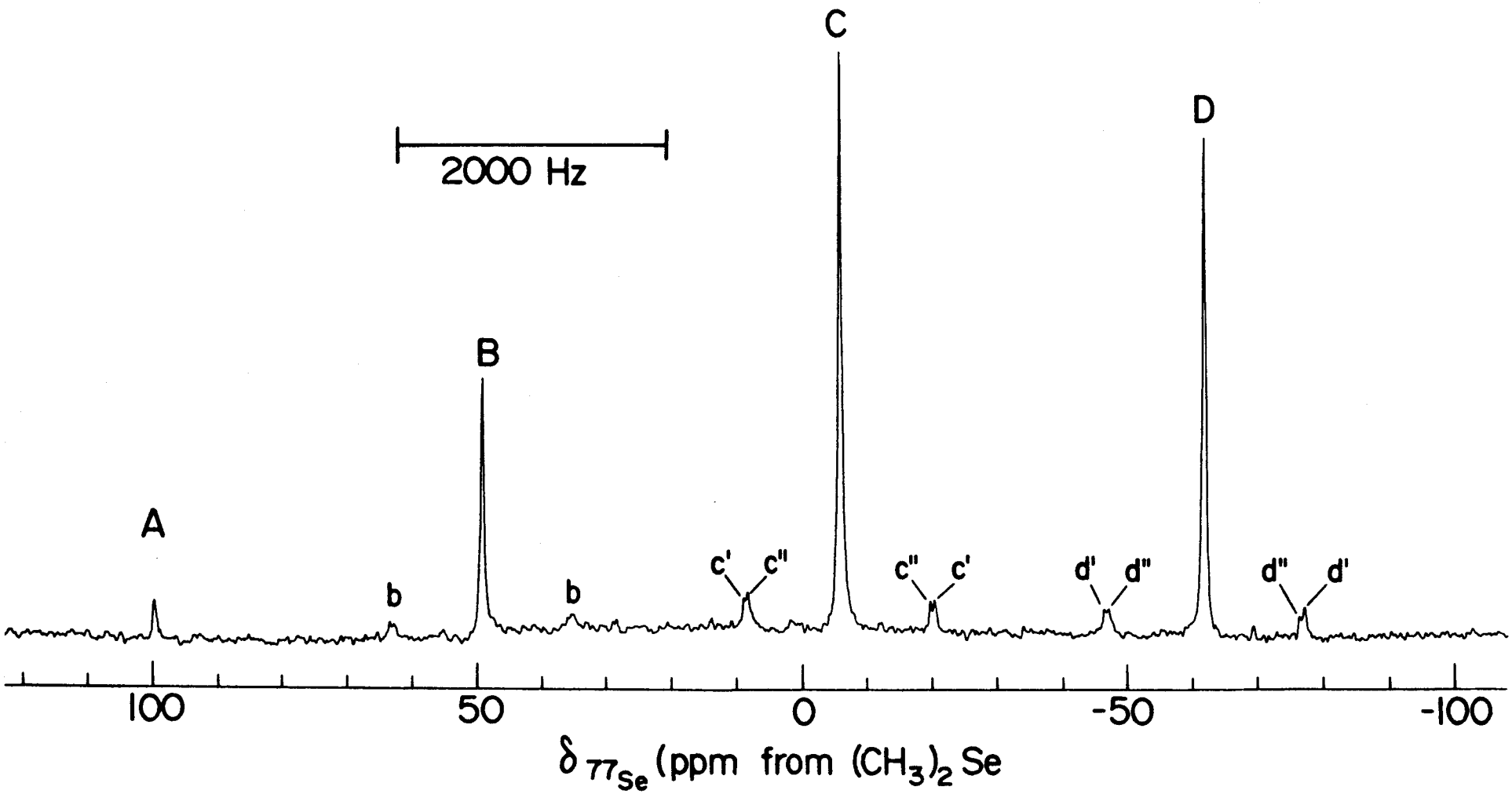

Fig. 6. ^{77}Se NMR spectrum for the $SnCh_4^{4-}$ series of anions, obtained at 47.70 MHz: (A) $SnTe_3Se^{4-}$; (B) $SnTe_2Se_2^{4-}$; (C) $SnTeSe_3^{4-}$; (D) $SnSe_4^{4-}$. Peaks labelled (b) denote $^{119,117}Sn$ satellites; (c') and (d') denote ^{119}Sn satellites while (c") and (d") denote ^{117}Sn satellites.

nuclei

3. relative satellite intensities in the ^{119}Sn spectra confirmed the assignments of (a) $SnTe_3Se^{4-}$, $SnTeSe_3^{4-}$ and $SnTe_2Se_2^{4-}$ as the ^{125}Te satellites in the $SnTe_3Se^{4-}$ should be approximately three times the intensity of the more closely spaced ^{77}Se satellites, while the opposite intensity distribution is expected for $SnTeSe_3^{4-}$ (Figs. 7 and8) and identical ^{77}Se and ^{125}Te satellite intensities expected for $SnTe_2Se_2^{4-}$ (Fig. 9) and (b) every member of the series by comparison of the integrated intensities of each satellite doublet with those calculated from the percent natural abundances of the ligand atoms.

The relevant chemical shifts, coupling constants and assignments for the $SnCh_4^{4-}$ series of anions are given in Table 4. Appendix A-3 contains a list of satellite doublet intensities (calculated and observed) for these anions.

Chemical Shift, δ

Nuclear shielding is usually discussed according to the terminology originated by Ramsey.[40] Both a diamagnetic (σ^d) and a paramagnetic (σ^p) component of the shielding constant (σ) may be defined such that

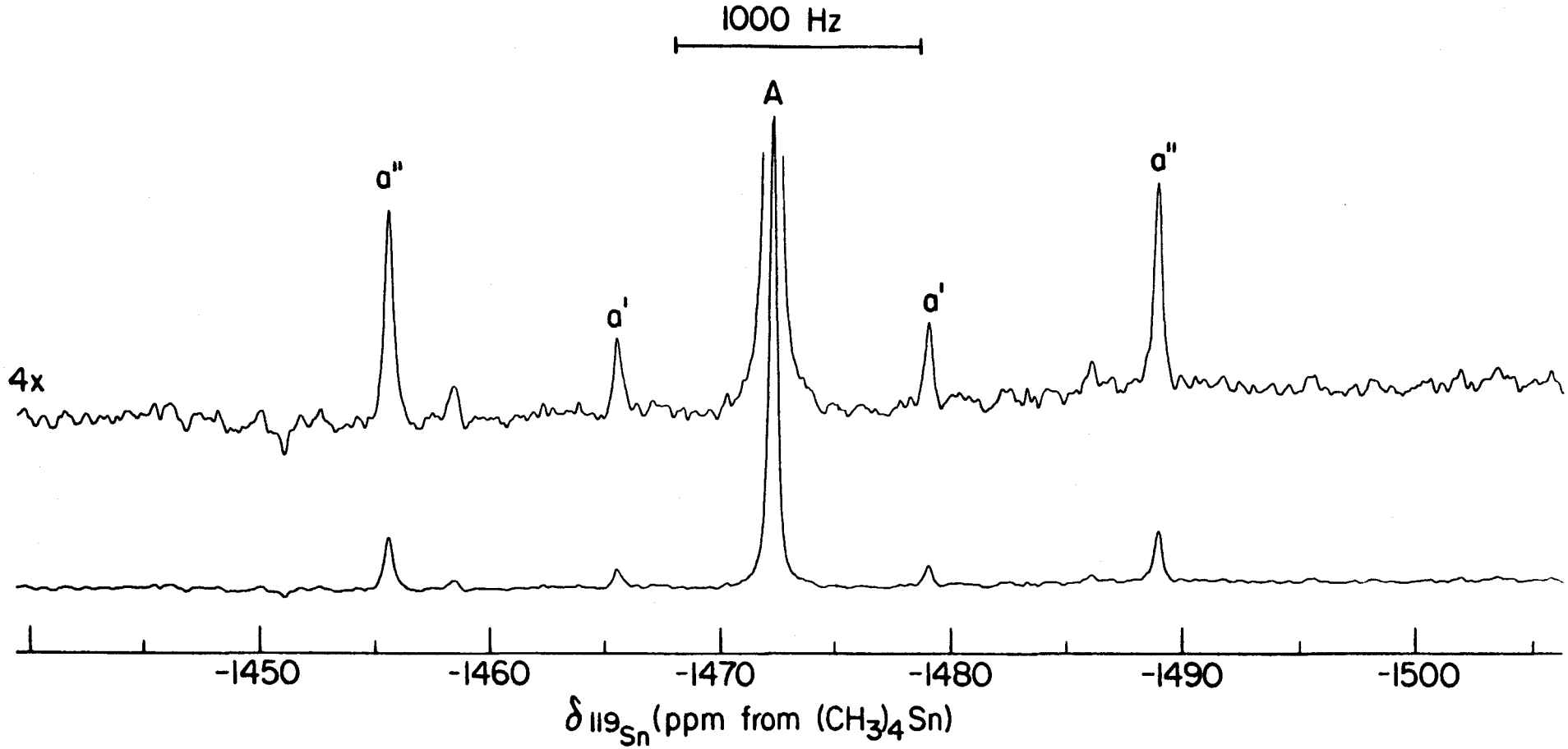

Fig. 7. ^{119}Sn NMR spectrum of the $SnTe_3Se^{4-}$ (A) anion, obtained at 93.27 MHz: (a') ^{77}Se satellites; (a") ^{125}Te satellites.

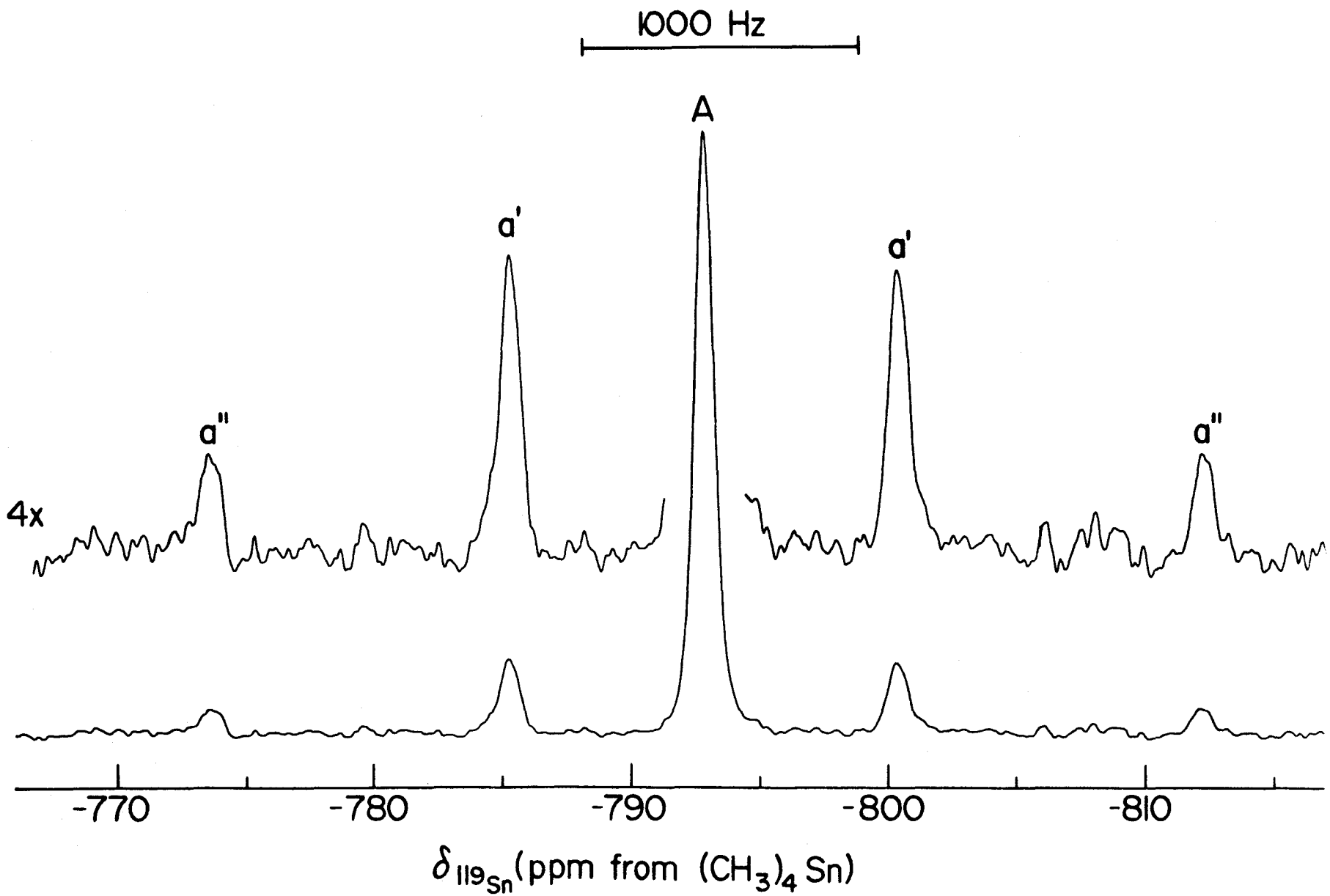

Fig. 8. ^{119}Sn NMR spectrum of the $SnTeSe_3^{4-}$ (A) anion, obtained at 93.27 MHz: (a') ^{77}Se satellites; (a") ^{125}Te satellites.

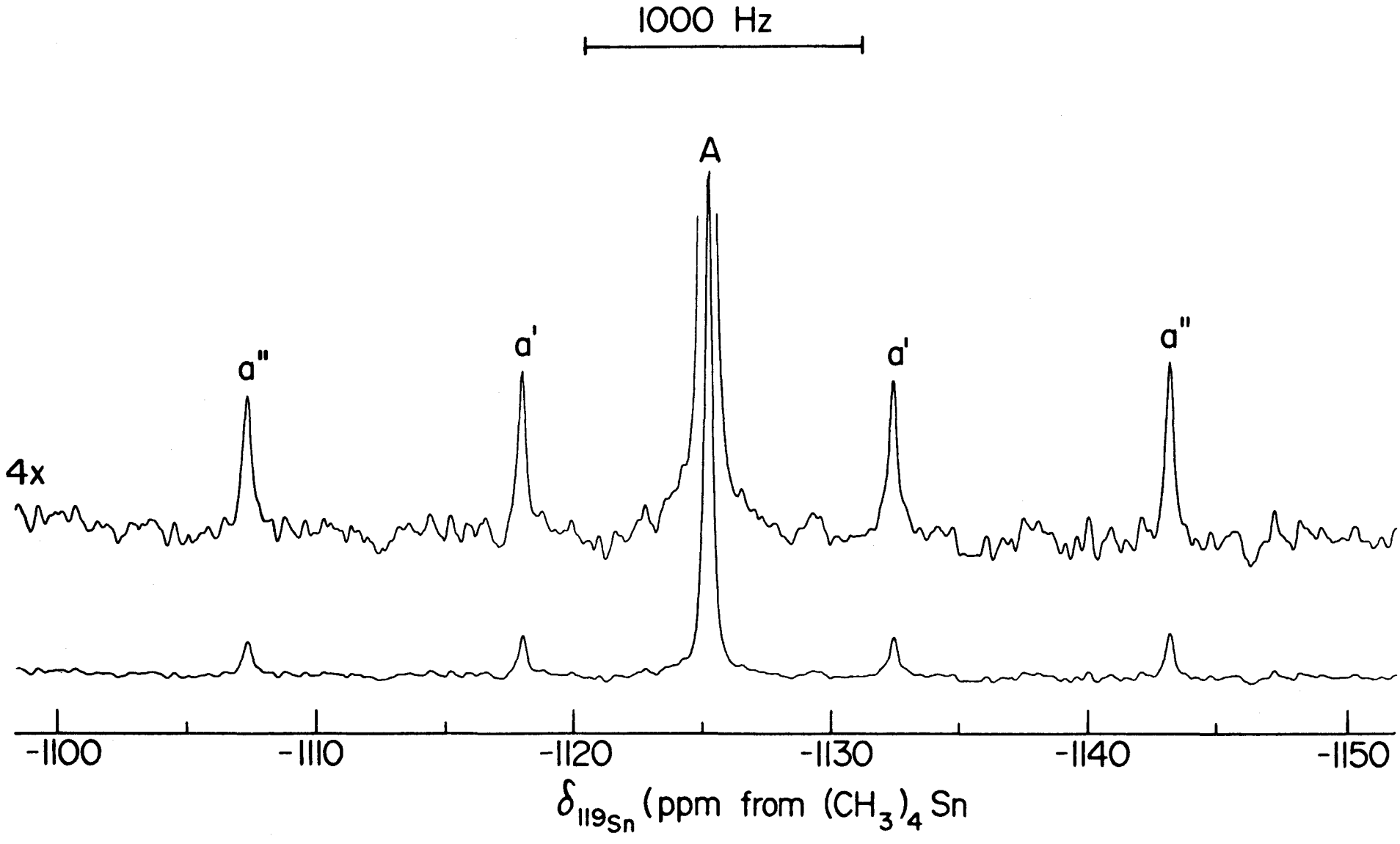

Fig. 9. ^{119}Sn NMR spectrum of the $SnTe_2Se_2^{4-}$ (A) anion, obtained at 93.27 MHz: (a') ^{77}Se satellites; (a") ^{125}Te satellites.

TABLE 4: NMR Parameters for the $SnCh_4^{4-}$ Anions

Anion	Chemical Shift, δ(ppm)						Coupling Constant, J(Hz)			
	^{119}Sn		^{125}Te		^{77}Se		^{119}Sn-^{125}Te	^{117}Sn-^{125}Te	^{119}Sn-^{77}Se	^{117}Sn-^{77}Se
	obs.	calc.	obs.	calc.	obs.	calc.				
$SnTe_4^{4-}$	-1823.6	-1812.7	-203.3	-199.3	-	-	2851	2727	-	-
$SnTe_3Se^{4-}$	-1472.3	-1475.3	-293.4	-298.3	99.6	101.3	3119	2981	1264	-
$SnTe_2Se_2^{4-}$	-1124.8	-1137.8	-395.1	-397.3	49.4	47.3	3340	3192	1341	1282
$SnTeSe_3^{4-}$	- 791.9	- 800.4	-499.4	-496.3	- 5.8	- 6.7	3571	3418	1402	1342
$SnSe_4^{4-}$	- 476.6	- 463.0	-	-	-61.9	-60.6	-	-	1463	1398

$$\sigma = \sigma^d + \sigma^p \qquad (2)$$

and where σ^d involves free rotation of electrons about the nucleus while σ^p describes the restriction to this rotation caused by other electrons and other nuclei in the molecule. From Table 4 it is clear that an increase in the electron-withdrawing ability of the ligand atoms attached to the central metal (i.e., Se is more electronegative than Te on the Pauling scale) leads to a decrease in the shielding of that nucleus. In principle this may be correlated with a change in the electron density on the central metal i.e. a diamagnetic contribution to shielding. However, the observed changes are too large to be accounted for by inductive effects alone, thus the paramagnetic term in equation (2) must be primarily responsible for the observed shifts of the tin nucleus. A progressive increase in shielding on replacing tellurium by selenium is observed for the ^{77}Se and ^{125}Te chemical shifts of these anions. This same trend was also observed for the $SnCh_3^{2-}$, $TlCh_3^{3-}$, $HgCh_2^{2-}$ and $CdCh_2^{2-}$ anions.[36] This is not what is expected based on simple inductive effects caused by substituting tellurium for selenium atoms in a particular geometry. As σ^d and σ^p are generally of opposite sign[41], one can see the dominance of the paramagnetic term in the chemical shift trends of the $SnCh_4^{4-}$ series of anions.

The ^{125}Te, ^{119}Sn and ^{77}Se chemical shifts are plotted vs the number of tellurium atoms (Fig.10) to illustrate their directly additive nature. Furthermore, each element was subjected to a linear least-squares regression analysis of the chemical shift data as a function of n, the number of tellurium atoms present in the anion. The equations governing the chemical shifts of the nuclei observed in the $SnCh_4^{4-}$ series are given below. Correlation factors, R,[42] of greater than 0.9994 for these

$SnSe_{4-n}Te_n^{4-}$: $\delta_{^{119}Sn} = -337.4n-463.0$ ppm (3)

($n \leq 4$) $\delta_{^{125}Te} = 99.0n-595.3$ ppm (4)

$\delta_{^{77}Se} = 54.0n-60.6$ ppm (5)

equations were calculated. All of the ^{119}Sn, ^{125}Te and ^{77}Se NMR assignments are supported by good agreement of the observed chemical shifts with those calculated above.

Coupling Constants, J and K

Table 4 also reveals that the spin-spin coupling constants along with the chemical shifts for the $SnCh_4^{4-}$ series are directly additive and an increase in the value of the coupling constant is observed on substituting selenium for tellurium. The spin-spin coupling constant originates from the interaction of nuclear spins with the surrounding electronic environment. One-bond coupling constants can be represented by equations (6) and (7) provided the Fermi contact mechanism is dominant,[43]

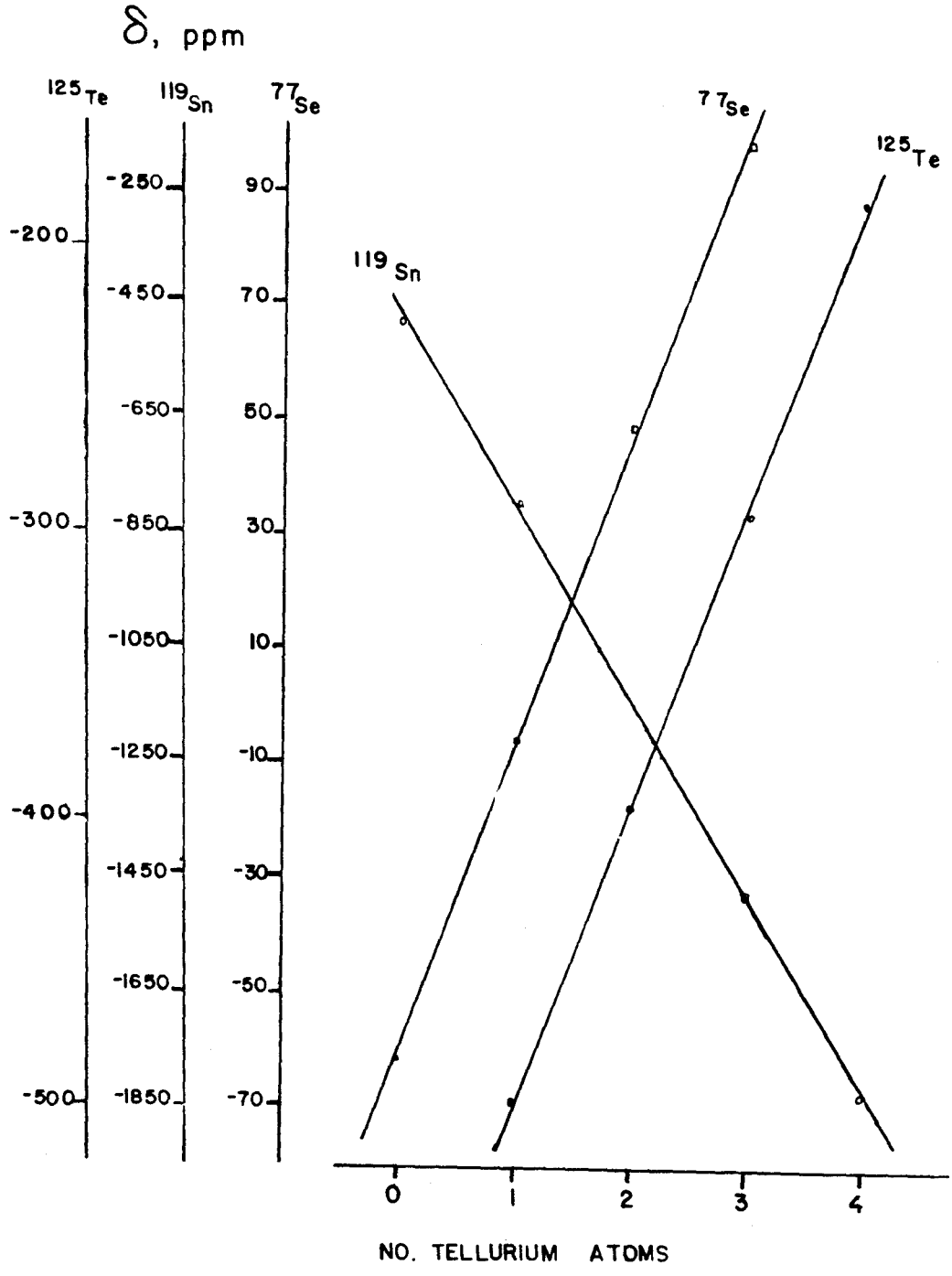

Fig. 10. Chemical shift trends for the $SnCh_4^{4-}$ series of anions.

$$^{1}J_{AB} = \frac{16\pi^2}{9h}\left(\frac{g\beta h}{2\pi}\right)^2 \gamma_A\gamma_B|\psi_{ns,A}(0)|^2|\psi_{ns,B}(0)^2\Pi_{AB} \quad (6)$$

$$\Pi_{AB} = 4 \sum_{i}^{occ.} \sum_{j}^{unocc.} \frac{C_{is,A}C_{js,A}C_{is,B},C_{js,B}}{(\varepsilon_j - \varepsilon_i)} \quad (7)$$

where all symbols have their usual meanings and/or values. $|\psi_{ns,A}(0)|^2$ and $|\psi_{ns,B}(0)|^2$ are the s-electron densities for the ns valence orbitals at the nuclei of atoms A and B, Π_{AB} is the mutual polarizability of the ns orbitals on A and B. $C_{n,A}$ and $C_{n,B}$ are the LCAO coefficients of the s-type atomic orbitals centred on A and B and $\varepsilon_i - \varepsilon_j$ represents the singlet excitation energy between the empty and filled molecular orbitals, i and j. Equation (6) demonstrates that the coupling constant, $^{1}J_{AB}$, is dependent on both the electronic and nuclear properties of the coupled nuclei. Specifically, coupling constants are proportional to the product of the magnetogyric ratios of the coupled nuclei. This nuclear dependence must be removed if comparison of spin-spin coupling constants for different molecules is to be useful. The reduced coupling constant, $^{1}K_{AB}$, gives a much better representation of the molecular electronic environment and is defined as follows,

$$^{1}K_{AB} = \frac{4\pi^2}{h\gamma_A\gamma_B} \; ^{1}J_{AB} \quad (8)$$

$$^{1}K_{AB} = \frac{4}{9}\mu_o{}^2\mu_B{}^2[|\psi_{ns,A}(0)|^2][|\psi_{ns,B}(0)|^2] \quad (9)$$

where $|\psi_{ns,A}(0)|^2$ and $|\psi_{ns,B}(0)|^2]$ are the valence shell s-electron densities at the nuclei A and B. The reduced

coupling constants for the $SnCh_4^{4-}$ series of anions are listed in Table 5.

Relativistic Corrections for Heavy Metals

Many of the physical and chemical anomalies associated with the heavier elements, particularly those nuclei in row six of the Periodic Table, can be rationalized if one considers the relativistic effects associated with these elements.[44,45] These effects are very important when considering hyperfine properties, since they depend on electronic wavefunctions near nuclei, where the electrons move very quickly.[46] Relativistic effects would then be expected to play an important role in any discussion of spin-spin coupling constants involving heavy metal elements. Assuming the contact interaction provides the largest contribution to spin-spin coupling, equation (9) clearly demonstrates that the reduced coupling constant, $^1K_{AB}$, is dramatically affected by the s-electron character in the hybridized orbitals on the atoms concerned. Since relativistic effects result in s-orbital contractions which, in turn, substantially increase the s-electron density[45] and hence the dominant Fermi contact terms in the indirect spin-spin coupling expression, some type of correction factor must be applied which takes into consideration these effects.

Gillespie et al.[47] have defined a "reduced density" coupling constant, $^1L_{AB}$, which factors out the

TABLE 5: Reduced Coupling Constants, ^1K, and Relativistically Corrected Reduced Coupling Constants, $^1K_{RC}$, for the $SnCh_4^{4-}$ Anions.

Anion	^1K [a]		$^1K_{RC}$ [a]	
	Sn-Te	Sn-Se	Sn-Te	Sn-Se
$SnTe_4^{4-}$	2.016	-	0.982	-
$SnTe_3Se^{4-}$	2.205	1.481	1.075	0.899
$SnTe_2Se_2^{4-}$	2.361	1.571	1.151	0.954
$SnTeSe_3^{4-}$	2.525	1.642	1.230	0.997
$SnSe_4^{4-}$	-	1.714	-	1.041

[a] ^1K and $^1K_{RC}$ are in SI units of $NA^{-2}m^{-3}$ when J is measured in Hz. All ^1K and $^1K_{RC}$ values are to multiplied by a factor of 10^{22}.

$|\psi_{ns,A}(0)|^2|\psi_{ns,B}(0)|^2$ dependence from equation (9). However, this attempt to account for the relativistic effects, by its very nature, renders the values of such calculations meaningless as representative of the spin-spin coupling between two nuclei. Spin-spin coupling, by definition, is due to the interaction between the nuclear spins of neighbouring nuclei via the valence electrons of the molecule,[37] therefore deleting the valence s-electron density terms from an expression defining a coupling constant in which the Fermi contact mechanism is dominant, effectively denies the mechanism through which coupling takes place. Pyykkö and Wiesenfeld[47] have tabulated values of the relativistic (and non-relativistic) hyperfine integral, υ_{-1}, related to $|\psi_{ns}(0)|^2$ by equation (10) for the main group elements using a sum-over-states, relativistically parameterized extended Hückel method with all parameters coming from relativistic or non-relativistic Hartree-Fock calculations along with Pyykkö's relativistic theory of spin-spin coupling[48]

$$|\psi_{ns}(0)|^2 = -\left(\frac{c}{2\pi}\right)\upsilon_{-1} \qquad (10)$$

the relativistic effect for a particular element can now be anticipated by considering the ratio $[|\psi_{ns}(0)|^2]_{rel.}/[|\psi_{ns}(0)|^2]_{non\text{-}rel.}$ The ratios for the elements contained in the $SnCh_4^{4-}$ series of anions are: Se = 1.155, Sn = 1.426 and Te = 1.439. Thus, for this series of anions, in the most extreme case of $^1K_{Sn-Te}$, a factor of 2.05 for a relativistic correction would

apply while in the least extreme case of $^1K_{Sn-Se}$ a factor of 1.65 would result. Obviously as the elements involved in spin-spin coupling increase in Z-value, the relativistic correction factors increase also. From our earlier work[36] a relativistic correction factor of 4.402 results when considering the $^1K_{Tl-Te}$ coupling in the trigonal-planar $TlTe_3^{2-}$ anion which when applied to $^1K_{Tl-Te}$ ($7.403 \times 10^{22} NA^{-2} m^{-3}$) gives a value of $^1K_{RC}$ ($1.682 \times 10^{22} NA^{-2} m^{-3}$). This "relativistically corrected" reduced coupling constant is now comparable to that found for the isostructural and isovalent $SnTe_3^{2-}$ anion ($1.562 \times 10^{22} NA^{-2} m^{-3}$) whereas the reduced coupling constant for $SnTe_3^{2-}$ ($3.206 \times 10^{22} NA^{-2} m^{-3}$) bears little resemblance to its thallium-tellurium counterpart. This demonstrates that great care must be taken when comparing coupling constants involving heavy elements with those involving lighter elements. It is therefore necessary to define a "relativistically corrected" reduced coupling constant according to equation (11)

$$(^1K_{AB})_{RC} = \left(\frac{|\psi_{ns}(0)|^2_{non\text{-}rel}}{|\psi_{ns}(0)|^2_{rel}}\right)_A \left(\frac{|\psi_{ns}(0)|^2_{non\text{-}rel}}{|\psi_{ns}(0)|^2_{rel}}\right)_B K_{AB} \quad (11)$$

and the values of $(^1K_{AB})_{RC}$ for the $SnCh_4^{4-}$ series of anions are given in Table 5. A listing of the relativistic and non-relativistic hyperfine integrals, υ_{-1}, along with the corresponding $|\psi_{ns}(0)|^2$ values is given in Table 6. As shown in Table 5, comparable reduced coupling constants, ^1K, are obtained within the tetrahedral tin series of anions, however,

TABLE 6: Parameters Used for the Determination of the Relativistic Effects Associated With Some Selected Heavy Metals.

	Element			
Parameter	Se	Te	Sn	Tl
υ_{-1},non-rel[a]	-0.7185781	-0.8745921	-0.5790300	-2.2430854
υ_{-1},rel[a]	-0.8300371	-1.2585161	-0.8255061	-0.7333231
$\lvert\psi_{ns}(0)\rvert^2$-non-rel[a]	15.672	19.075	12.629	15.994
$\lvert\psi_{ns}(0)\rvert^2$-rel[a]	18.103	27.442	18.004	48.923
$\frac{\lvert\psi_{ns}(0)\rvert^2_{rel}}{\lvert\psi_{ns}(0)\rvert^2_{non-rel}}$	1.155	1.439	1.426	3.059

[a] Hyperfine integral, υ_{-1}, values taken from reference 46.

[b] $\lvert\psi_{ns}(0)\rvert^2$ values are given in units of a_o^{-3}.

considerable differences in ^{1}K values for homologous series of anions possessing different central atoms have been observed.[36] In such instances the "relativistically corrected" reduced coupling constant, $^{1}K_{RC}$, allows useful comparisons of the bonding in homologous series to be made.

CHAPTER IV

PREPARATION AND NMR SPECTROSCOPIC STUDIES OF THE $Sn_2Se_6^{4-}$ ANION

INTRODUCTION

The two ternary alloys $KSnTe_2$ and $KSnSe_2$ were prepared and extracted with en in the presence of crypt producing deep orange-brown and orange colored solutions, respectively. These solutions were investigated by ^{119}Sn, ^{125}Te and ^{77}Se NMR spectroscopy and were found to primarily contain the $SnTe_3^{2-}$ and $SnSe_3^{2-}$ anions. As the dimer of $SnTe_3^{2-}$, $Sn_2Te_6^{4-}$, has recently been structurally characterized by Haushalter and co-workers[49] there exists a distinct possibility that the $SnTe_3^{2-}$ anion does not maintain its trigonal-planar structure in the solid state. A complete discussion of findings in this regard is presented in a later section. Attempts to produce the $Sn_2Te_6^{4-}$ anion in solution have, to this point, failed to yield any conclusive evidence. However, efforts to produce the hitherto unknown selenium analog, $Sn_2Se_6^{4-}$, have been successful.

RESULTS AND DISCUSSION

Anions Extracted From $KSnTe_{2-x}Se_x$ (x = 0,2) Alloys

Initially, extraction of the ternary alloy $KSnSe_2$ with en and crypt followed by the addition of an excess of the alloy gave a yellow-green colored solution. Two broad resonances in an approximate 2:1 ratio with possible satellite structures were observed in the ^{77}Se room temperature NMR spectrum, while a single broad resonance was seen in the ^{119}Sn NMR spectrum. If the $Sn_2Se_6^{4-}$ anion was indeed present in solution and was isostructural with B_2H_6 and $Sn_2Te_6^{4-}$,[49] then two different selenium environments in a 2:1 ratio representing the four terminal and two bridging selenium atoms as shown in structure (I) would be expected in the ^{77}Se NMR spectrum. The preliminary results stated above were therefore very encouraging

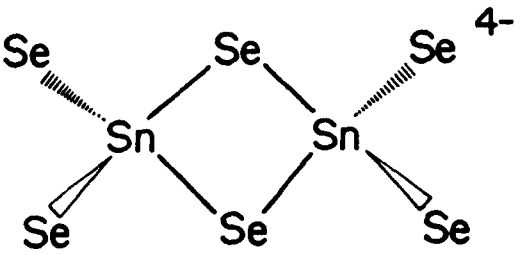

(I)

and it was decided to repeat the NMR experiment at low temperature. Unfortunately, the minimum temperature this particular NMR sample could be recorded at was 278K, but additional structural information was forthcoming. The ^{119}Sn resonance

at -396.6 ppm was accompanied by two sets of ^{77}Se satellites (Fig. 11) suggesting that a slow exchange process is responsible for the broadening of the NMR spectra at room temperature. As expected, the terminal selenium atoms are more shielded than the bridging selenium atoms since formally the negative charge in structure (I) would reside on the terminal selenium atoms. Interestingly, two intense peaks were observed in the ^{77}Se NMR spectrum located either side of the terminal selenium signal for $Sn_2Se_6^{4-}$. Their identity has not, at this point, been established.

The spin-spin coupling constants are consistent with those values measured from the ^{77}Se NMR spectrum (Fig. 12) with the smaller $J_{^{119}Sn-^{77}Se}$ value corresponding to tin coupled to the bridging selenium atoms. The smaller coupling constant indicates a weaker bonding interaction in the bridging selenium-tin bonds than the terminal selenium-tin bonds as would be expected for the assumed structure.[49] Both coupling constants are significantly smaller than those found for the $SnCh_4^{4-}$ and $SnCh_3^{2-}$ series of anions again reflecting the difference in the bonding of this species to the tetrahedrally-bonded anions. The relevant chemical shifts, coupling constants and assignments for the $Sn_2Se_6^{4-}$ dimeric species are given in Table 7. The reduced coupling constants are 2.380 and $1.044 \times 10^{22} NA^{-2}m^{-3}$ for the terminal and bridging tin-selenium bonds, respectively, while the relativistically cor-

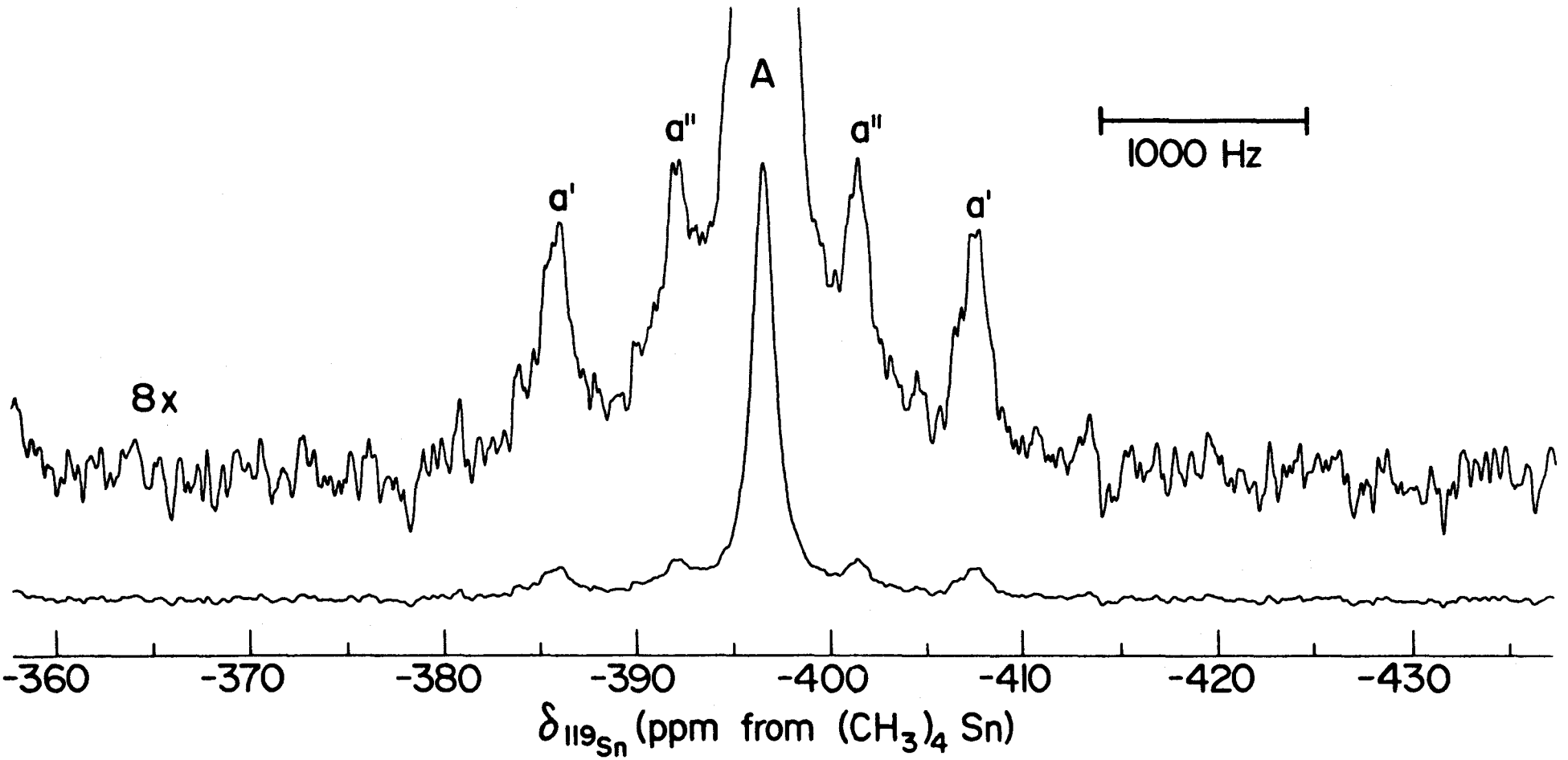

Fig. 11. ^{119}Sn NMR spectrum of the $Sn_2Se_6^{4-}$ (A) anion, obtained at 93.27 MHz: (a') ^{77}Se satellites for the terminal selenium atoms; (a'') ^{77}Se satellites for the bridging selenium atoms.

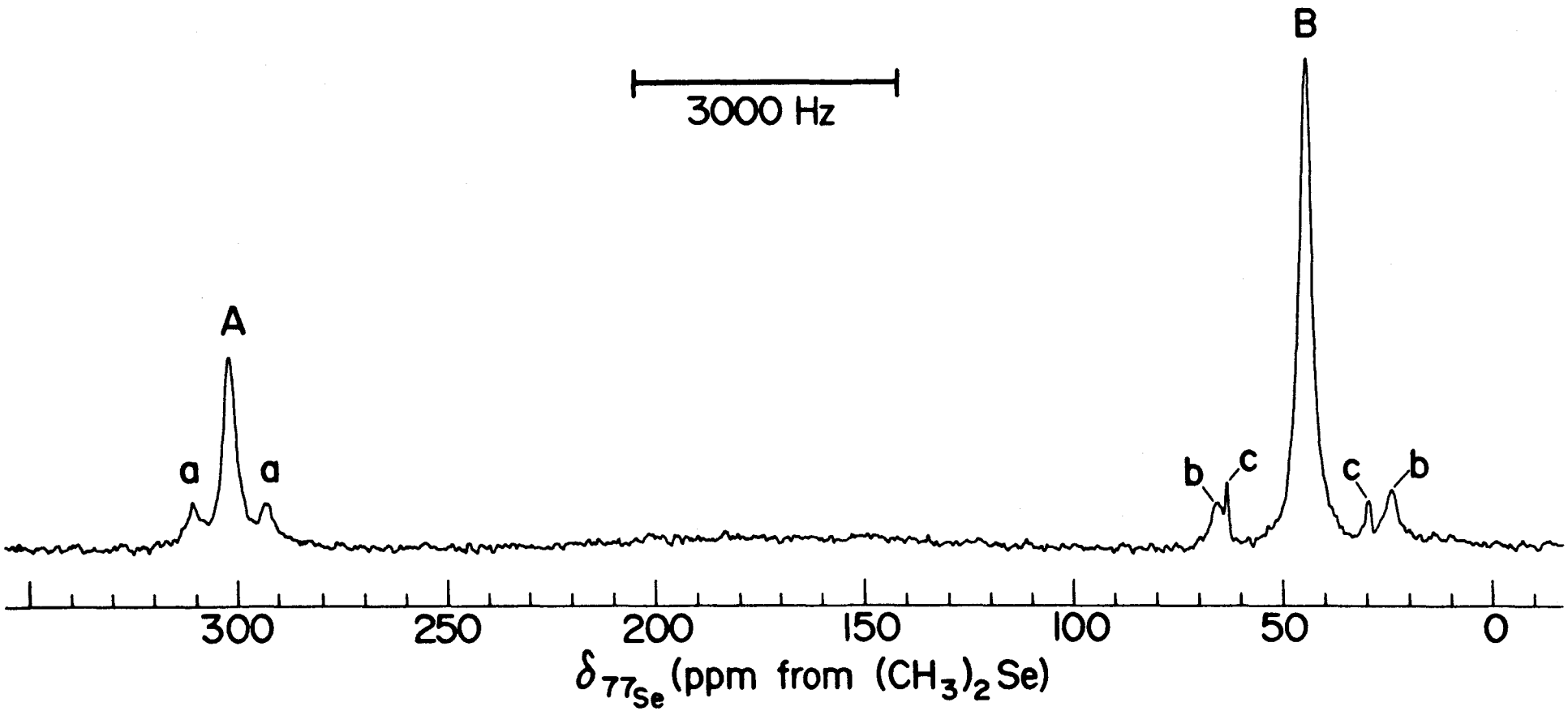

Fig. 12. ^{77}Se NMR spectrum of the $Sn_2Se_6^{4-}$ anion, obtained at 47.70 MHz showing the bridging seleniums on tin (A) and the terminal seleniums on tin (B); (a) and (b) denote $^{117,119}Sn$ satellites; (c) unknown resonances.

TABLE 7: NMR Parameters for the $Sn_2Se_6^{4-}$ Anion

Temperature (K)	Chemical Shift, δ(ppm)		Coupling Constant, J(Hz)
	^{119}Sn	^{77}Se[a]	$^{117/119}Sn - ^{77}Se$[b]
298	-396.6	48.1(t,300)[c]	2002 (t)
		308.1(b,360)	812 (b)
278	-396.6	45.1(t,160)	2032 (t)
		301.7(b,175)	891 (b)

[a] Additional ^{77}Se resonances found at 63.4 ppm and 29.7 ppm.

[b] $^{117/119}Sn$-^{77}Se coupling constants taken from the ^{119}Sn NMR spectrum.

[c] "t" and "b" in parentheses refer to terminal and bridging selenium atoms, respectively, while the numerical value represents the linewidth, $\Delta\nu_{\frac{1}{2}}$, associated with a given signal.

rected reduced coupling constants are 1.445 and $0.634 \times 10^{22} NA^{-2} m^{-3}$. $^1K_{RC}$ for the bridging selenium atoms is approximately one-half of the value for the terminal selenium atoms, and is therefore indicative of the anticipated bond orders for the bridging tin-selenium bonds. The $^1K_{RC}$ value for the terminal tin-selenium bonds is considerably larger than the tin-selenium $^1K_{RC}$ in $SnSe_4^{4-}$ and is, in fact, very close to that observed in $SnSe_3^{2-}$ ($1.459 \times 10^{22} NA^{-2} m^{-3}$).[36] This only serves to re-amplify the fact that tin does not exhibit sp^3 hybridization in the dimer.

Obviously improved resolution of the NMR spectra was desirable, however when the same experimental approach was carried out replacing en with liquid NH_3 the tin dimer was not soluble enough to be able to observe an NMR spectrum of good quality. Two sharp resonances at -88.5 ppm ($\Delta\nu_{\frac{1}{2}} \sim 50$ Hz) and -429.25 ppm ($\Delta\nu_{\frac{1}{2}} = 25$ Hz) of approximate equal intensity were observed in the ^{77}Se NMR spectrum, but were not assigned due to the lack of ^{117}Sn and ^{119}Sn satellites on these signals. The signal-to-noise ratio was rather poor (even after $\sim$ 250,000 scans) due to the relatively dilute nature of the sample. If these signals do, in fact, belong to the $Sn_2Se_6^{4-}$ anion then there is a huge solvent effect associated with the ^{77}Se chemical shifts of this anion. A variety of other solvents were also tested but with no success.

It should be noted that NMR evidence for the presence of small amounts of $SnSe_3^{2-}$ ($\sim$10% of total) was found in both

the ^{77}Se and ^{119}Sn NMR spectra of the above solutions. In order to determine whether or not the formation of $Sn_2Se_6^{4-}$ proceeds via the dimerization of $SnSe_3^{2-}$, a yellow-green solution containing the dimer was produced and isolated from any remaining alloy residue. To this solution was added a stoichiometric amount of crypt resulting in an orange solution which, when investigated by ^{77}Se and ^{119}Sn NMR spectroscopy, was found to contain only the monomeric species $SnSe_3^{2-}$ (equations (12) and (13)). It is clear

$$KSnSe_2 + en + crypt \xrightarrow{5\ days} SnSe_3^{2-} \qquad (12)$$

$$SnSe_3^{2-} \underset{\text{crypt (excess)}}{\overset{KSnSe_2\text{(excess)}}{\rightleftharpoons}} Sn_2Se_6^{4-} \qquad (13)$$

that the addition of excess alloy to a solution containing $SnSe_3^{2-}$ and cryptated K^+ ions results in a build-up of uncomplexed K^+ ions in solution. Any free alkali metal cation would then form ion-pairs with the monomeric $SnSe_3^{2-}$ anion, thereby reducing the electronic repulsions between anions and promoting formation of the dimer as shown below

$$SnSe_3^{2-}, nK^+ \rightarrow Sn_2Se_6^{4-}, mK^+ + (n-m)K^+ \qquad (14)$$

where n is assumed to have a maximum value close to two.

When $KSnSe_2$ was extracted in en without crypt the resulting yellow-green solution was found to contain some of the dimer, $Sn_2Se_6^{4-}$, but the NMR signals were very broad and the signal-to-noise ratio was also poor. In our laboratory we have discovered that the absence of any cryptating agent

in the solutions of these anions often precludes their detection by NMR spectroscopy or results in very broad NMR resonances. This is thought to be due to very strong ion-pair effects and slow exchange processes occuring. This is nicely illustrated by the behaviour of the Te_3^{2-} anion studied by Már Björgivinsson in this laboratory. A solution of Te_3^{2-} in en results in a single broad line ($\Delta\nu_{\frac{1}{2}} \sim 3000$ Hz) observed at -326 ppm in the ^{125}Te NMR spectrum. This solution was recovered and a stoichiometric amount of crypt was added. The ^{125}Te NMR spectrum of the resulting solution consisted of two sharp peaks in a 2:1 ratio at -298 and -372 ppm, respectively. These resonances were assigned to the known V-shaped anion Te_3^{2-}.[50] The formation of ion-pairs in the non-cryptated solution would facilitate the intermolecular exchange of tellurium environments in Te_3^{2-}, hence the observed broad NMR line. However, complexation of the alkali metal reduces the liklihood of ion-pairs in solution. Since the interaction between negatively charged ions is decreased, so too is the intermolecular exchange, which results in two sharp NMR peaks corresponding to the two terminal and one bridging tellurium environment(s) of Te_3^{2-}.

In addition, three other signals to low frequency of $SnSe_3^{2-}$ and of low concentration (1-5% of total) were observed in ^{119}Sn NMR spectrum of the solution extracted from the $KSnSe_2$/en/crypt mixture. Two of these signals centered at -338.8 and -364 ppm were found to be very interesting since

they displayed satellites corresponding to coupling constants of 159 Hz and 348 Hz, respectively. Since these signals were located far off resonance no accurate determination of the satellite to central peak intensity ratio could be made. However, the small coupling constants are indicative of tin cluster species, for example, Rudolph[34] reports a value of 254 Hz for the ^{119}Sn-^{117}Sn spin-spin coupling in the fluxional Sn_9^{4-} cluster anion. No comparable species were found in the ^{77}Se NMR spectrum of the same solution. Several additional peaks were observed though, the most intense being three sharp signals at 59.8 ppm, 53.5 ppm and 42.3 ppm with no apparent satellite structures.

CHAPTER V

PREPARATION AND NMR SPECTROSCOPIC STUDIES OF THE REACTION OF $Sn(II)Cl_2$ WITH Te_2^{2-}, AND SOLUTIONS EXTRACTED FROM TERNARY Na/Sn/Te ALLOYS.

INTRODUCTION

Investigation of the en solution extracted from the ternary NaSnTe alloy with crypt resulted in the identification of the $SnTe_4^{4-}$ anion. However, two additional sharp NMR signals were observed in the ^{125}Te NMR spectrum at -435 and -618 ppm with the less shielded resonance flanked by what appeared to be a weak set of tin satellites. Investigation of the same solution by ^{119}Sn NMR spectroscopy failed to yield any corresponding signal due to the dilute nature of these species ($\sim$ 13% and 3% of total intensities, respectively). It was therefore decided to make a very concentrated sample extracted from the same alloy in the hopes of increasing the concentrations of the weaker signals to a point were spin-spin coupling constants could be measured. The ^{125}Te NMR spectrum again contained the $SnTe_4^{4-}$ anion along with the two previously documented unassigned resonances as well as a small peak at -290 ppm. The signal located at -435 ppm was put on resonance and $^{119,117}Sn$ satellites were observed. The magnitudes of the ^{119}Sn-^{125}Te and ^{117}Sn-^{125}Te coupling constants were found to be 4340 Hz and 4144 Hz, respectively, which is comparable to those values of $^1J_{^{119}Sn-^{125}Te}$ and $^1J_{^{117}Sn-^{125}Te}$ (4300-4800 Hz)[36] measured from the

^{119}Sn and ^{125}Te NMR spectra of the trigonal-planar $SnCh_3^{2-}$ series of anions. The ratio of the intensities of the satellite peak to the central peak indicated that the tellurium environment was bonded to a single tin atom. A corresponding resonance was observed in the ^{119}Sn NMR spectrum at -1216 ppm which is just slightly more shielded than δ ^{119}Sn for $SnTe_3^{2-}$ (-1170 ppm).[36] Furthermore, the integrated satellite intensities show that the tin atom is coordinated to three equivalent tellurium atoms. An additional peak of intermediate concentration ($\sim$ 25% of total) was also observed at -1041 ppm. Unfortunately, the signal located at -618 ppm in the ^{125}Te NMR spectrum was still not strong enough for satellites to be observed.

RESULTS AND DISCUSSION

NMR Investigations of Solutions Extracted from $NaSn_2Te_{1.5}$ and $NaSn_{1.5}Te$ Alloys

In order to produce the as-of-yet unassigned signals found in solutions extracted from the NaSnTe alloy independently, two new alloys of composition $NaSn_2Te_{1.5}$ and $NaSn_{1.5}Te$ were prepared and extracted in en with crypt. The ^{125}Te NMR spectrum of the orange-brown solution extracted from $NaSn_2Te_{1.5}$ alloy yielded a variety of signals ranging from -200 to -1000 ppm (Fig. 13). Table 8 contains data for all the NMR signals found in these solutions. Two intense signals of almost equal intensity were observed with δ ^{125}Te values of

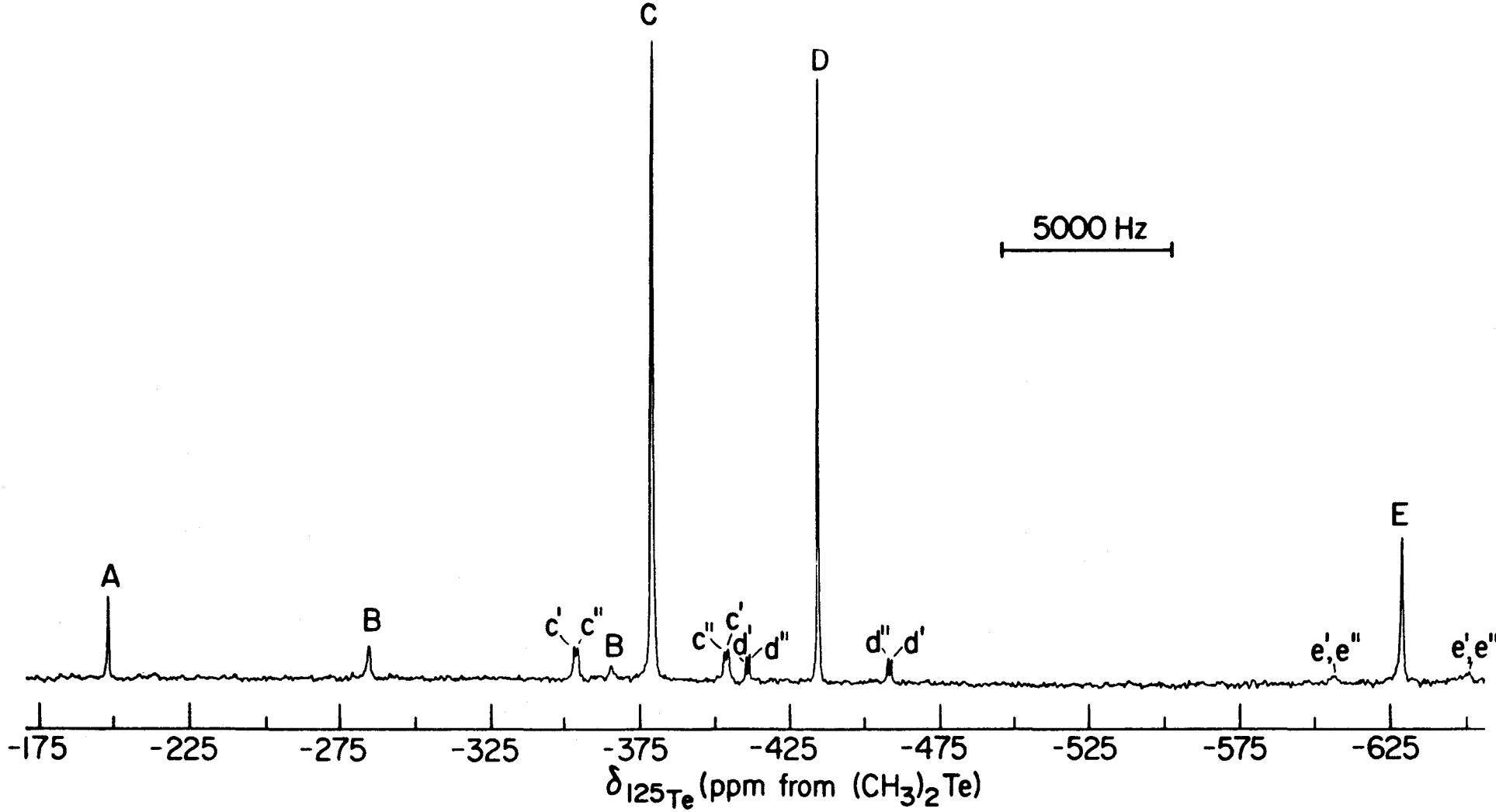

Fig. 13. ^{125}Te NMR spectrum, obtained at 78.92 MHz, of the solution extracted from the $NaSn_2Te_{1.5}$ alloy: (A) $SnTe_4^{4-}$; (B) Te_3^{2-}; (C) $SnTe_3^{2-}$; (D) and (E) are unassigned signals. Peaks labelled (c'), (d') and (e') denote ^{119}Sn satellites while those labelled (c'), (d") and (e") denote ^{117}Sn satellites.

-385 and -432 ppm. Both signals were accompanied by a pair of $^{119,117}Sn$ satellite doublets. The less shielded resonance had a ^{125}Te chemical shift identical to that of $SnTe_3^{2-}$ and the $^{119,117}Sn$-^{125}Te spin-spin coupling constants confirmed the identity of this signal as $SnTe_3^{2-}$. The other intense signal at -432 ppm corresponded to one of the unidentified peaks observed in the NaSnTe extracts since both $\delta\ ^{125}Te$ and $^1J_{117,119Sn-^{125}Te}$ values were the same. The major difference in the ^{125}Te NMR spectra of the NaSnTe and $NaSn_2Te_{1.5}$ solutions is that the former contains primarily the $SnTe_4^{4-}$ anion along with the unassigned resonances, while the latter contains the $SnTe_3^{2-}$ anion. In both alloys tin is nominally tin(I), i.e., $Na^+Sn^+(Te^{2-})$ and $Na^+(Sn^+)_2(Te^{2-})_{1.5}$. Disproportionation of the tin(I) in each case can be represented by equation (15).

$$4Sn^+ \rightarrow Sn^{4+} + 3Sn \qquad (15)$$

This leads to ratios of Te^{2-}/Sn^{4+} of four and three, in agreement with the major products, $SnTe_4^{4-}$ and $SnTe_3^{2-}$, obtained in each extraction. The signal at -618 ppm in the ^{125}Te NMR spectrum was much more intense than found in the solutions of the NaSnTe extracts. A pair of $^{119,117}Sn$ satellite doublets was observed (Fig. 14) with $^1J_{119Sn-^{125}Te}$ equal to 4034 Hz which is of similar magnitude to the spin-spin couplings of the $SnCh_3^{2-}$ series of anions as well as the unassigned resonance at -432 ppm. Measurement of the satellite intensities

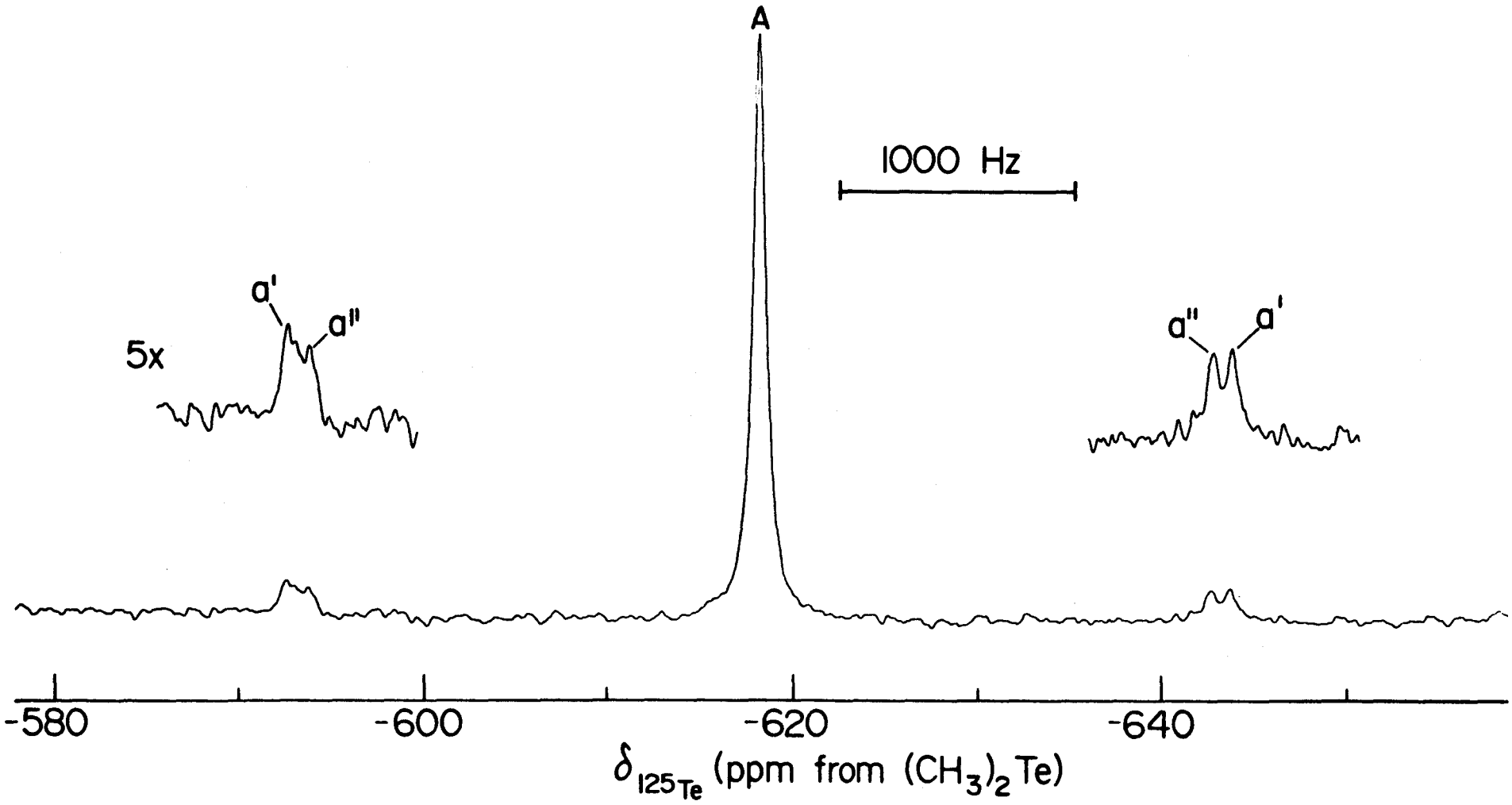

Fig. 14. ^{125}Te NMR spectrum, obtained at 78.92 MHz, for the unassigned resonance (A): (a') ^{119}Sn satellites; (a") ^{117}Sn satellites.

confirmed that once again, a single tin atom was coordinated to tellurium.

Four other signals were observed in the ^{125}Te NMR spectrum of the $NaSn_2Te_{1.5}$/en/crypt solutions at -1012, -370, -294 and -208 ppm with approximate concentrations less than 5% of the total except for the signal at -208 ppm, which was 13% of the total. The least shielded resonance, was reasonably sharp and had a chemical shift very similar to that of $SnTe_4^{4-}$ (-203 ppm) but since no tin satellite structure could be detected, assignment of this signal cannot be made unambiguously. The most shielded signal did not correspond to any known species and showed no evidence of satellites, and thus was not assigned. Conversely, the remaining two signals were slightly more broad than the others and appeared to have an intensity ratio of 2:1. On closer inspection, it was discovered that the chemical shifts and intensity ratio were virtually identical to those observed in the ^{125}Te NMR spectrum of the polychalcogenide anion, Te_3^{2-},[51]. This was the first example of a polychalcogenide anion in solution along with tin-containing species in this work.

The ^{119}Sn NMR spectrum of the above solution was found to contain three signals at -1170, -1215 and -1041 ppm. The least shielded resonance was also seen in the ^{119}Sn spectrum of the ternary NaSnTe alloy extracts and, as in the earlier investigation, was not assigned. The signals at -1170 and -1215 ppm, with an approximate intensity ratio of

3:2, were both flanked by a set of ^{125}Te satellites. The satellite-to-central peak intensity ratios revealed that both tin environments were coupled to three equivalent tellurium atoms. The chemical shift and coupling constant of the -1170 ppm peak were identical to those observed for the $SnTe_3^{2-}$ anion. The coupling constant corresponding to the signal at -1215 ppm matched that measured from the ^{125}Te spectrum for the unassigned resonance at -432 ppm. No tin signal accompanied by ^{125}Te satellites and a spin-spin coupling constant corresponding to that measured from the ^{125}Te spectrum of the remaining unassigned peak at -613 ppm was observed over a chemical shift range of -1000 to -2200 ppm. The ^{119}Sn and ^{125}Te chemical shifts along with the $^{119,117}Sn$-^{125}Te spin-spin coupling constants for this species are tabulated in Table 8.

Extraction of the $NaSn_{1.5}Te$ alloy in en with crypt produced a reddish-orange solution which when investigated by ^{125}Te NMR spectroscopy revealed a total of four signals, two of low concentration (<10% of total) and two of approximate equal concentration (~45% of total, each). The two most intense peaks at -203 and -432 ppm belong to the same species observed initially in the ^{125}Te NMR spectrum of the NaSnTe extracts, only in this case $SnTe_4^{4-}$ occurs in about the same concentration as the unidentified species which resonates at -432 ppm. The remaining two signals at -184 and -613 ppm are unassigned, although the more shielded signal is the

same species which has been observed in the aforementioned tin solutions at the same chemical shift. When the same approach for the disproportionation of tin in this alloy is taken as for the NaSnTe and $NaSn_2Te_{1.5}$ alloys, a Ch^{2-}/Sn^{4+} ratio of about 4 results. It is not surprising therefore that both NaSnTe and $NaSn_{1.5}Te$ extracts give the $SnTe_4^{4-}$ anion while $NaSn_2Te_{1.5}$ gives the $SnTe_3^{2-}$ anion, along with the additional signals at -432 and -613 ppm. The "relativistically corrected" reduced coupling constants for these two signals, 1.497 and 1.389 x 10^{22} NA^{-2} m^{-3}, respectively, are considerably larger than the value calculated for $SnTe_4^{4-}$ (0.982 x 10^{22} NA^{-2} m^{-3}) with sp^3 hybridization of tin, but are of the same magnitude as $^1K_{RC}$ for $SnTe_3^{2-}$ (1.562 x 10^{22} NA^{-2} m^{-3}) with sp^2 hybridization of the central metal.

It is interesting to note that the ever-present signals (-432 and -613 ppm) in the ^{125}Te NMR spectra of these solutions always occur together and are always observed in an approximate intensity ratio of 3 or 4/1. This suggests that these two resonances belong to the same species in solution or are two distinct species, perhaps the result of the decomposition of some other tin compound. The most probable dinuclear tin species such as $Sn_2Te_6^{4-}$ and $Sn_2Te_7^{6-}$ do not fit the observed NMR data. Observation of the ^{119}Sn resonance which corresponds to the observed ^{125}Te signal at -613 ppm would at least provide the number of tellurium atoms

TABLE 8: NMR Parameters for the Extracted Solutions of $NaSnTe$, $NaSn_2Te_{1.5}$ and $NaSn_{1.5}Te$

Alloy	Chemical Shift, δ(ppm) ^{119}Sn	^{125}Te	Coupling Constant, J(Hz) ^{119}Sn-^{125}Te	^{117}Sn-^{125}Te
NaSnTe	-1216	-435	4340(1.497)[a]	4144
	-1824	-203	2851(0.982)	2727
		-290		
		-618		
$NaSn_2Te_{1.5}$	-1041	-208		
		-294		
		-370		
	-1170	-385	4535(1.562)	4335
	-1215	-432	4345(1.497)	4152
		-613	4034(1.389)	3857
		-1012		
$NaSn_{1.5}Te$		-184		
		-203	2851	2728
		-432	4344	4144
		-613		

[a] The numbers in parentheses are the "relativistically corrected" reduced coupling constants, $^1K_{RC}$ in units of $NA^{-2}\ m^{-3}$. Each $^1K_{RC}$ value is to be multiplied by a factor of 10^{22}.

that the tin atom in this species is coordinated. New alloys containing both tellurium and selenium might lead to an analogous mixed series of anions and could, in turn, shed some light on this system. Both of the extracted alloy solutions, at present, have produced some crystalline material and therefore attempts at growing crystals from these solutions should be made. However, these crystals might turn out to be stable species such as $SnTe_4^{4-}$,[28] Te_3^{2-},[50] and Te_4^{2-},[49,66] which are well-documented, thus more information on these solutions is desirable before any crystallographic study is made.

The initial problem of producing reasonably concentrated solutions containing the two interesting and unidentified species as major species has obviously been solved. The identification of these species has proved much more difficult and requires more time and effort. It is reasonable to believe that these species might be intermediates involved in the complex solution chemistries of the $SnCh_3^{2-}$ and $SnCh_4^{4-}$ anions as well as the dimeric $Sn_2Se_6^{4-}$ anion, thus the impetus for continuation of this work.

Reaction of $SnCl_2$ and Te_2^{2-}

A dinuclear lead series of anions, $Pb_2Se_{3-n}Te_n^{2-}$, possessing structures based on a trigonal bipyramid with the chalcogen atoms occupying the equatorial positions and bonded to two lead atoms in the apical positions has recently been

identified through multinuclear magnetic resonance spectroscopy and X-ray crystallography in this laboratory.[51] No similar tin species, to this point, has been observed which is not surprizing since the principle stable oxidation state of lead is +2 while for tin it is +4. For a comparable tin species to exist, tin would have to be present in a +2 oxidation state. It was therefore decided to try a reaction with a tin(II) compound and Te_2^{2-}. When anhydrous $Sn(II)Cl_2$ was reacted with a violet-blue solution containing Te_2^{2-} in a 1:3 ratio, upon contact a reddish-orange colored solution was formed. As more of the Te_2^{2-} solution reacted with the $SnCl_2$ the solution became a deeper red color. Along with this reaction was the appearance of a relatively large amount of white crystalline material thought to be KCl which is insoluble in en. This reaction was allowed to go for several days during which time the solution became deeper reddish-brown in color. During concentration of this sample for NMR study, a yellow coating appeared on the sides of the NMR tube. Investigation of this solution by ^{125}Te NMR revealed a single broad resonance ($\Delta\nu_{\frac{1}{2}} \sim 600$ Hz) at approximately -317 ppm. This signal was assigned to the V-shaped Te_3^{2-} anion as the weighted average chemical shift for the cryptated Te_3^{2-} solution of -323 ppm corresponded well with the chemical shift quoted above.

Obviously the Te_3^{2-} anion is a very stable species in these solutions, therefore it was decided to stop the reaction

of $SnCl_2$ with Te_2^{2-} and isolate a suitable NMR sample before any significant amount of Te_3^{2-} were formed. The reaction was halted after about ½-hour, and the orange-red colored solution investigated by ^{125}Te NMR. Unfortunately, not a single resonance was observed. This sample was then placed in a glove bag purged with dry $N_2(g)$ and a stoichiometric amount of crypt added. This time the ^{125}Te NMR spectrum was found to contain one broad signal ($\Delta\nu_{\frac{1}{2}} \sim 700$ Hz) at -385 ppm and two very sharp peaks of equal intensity located at -27 and -85 ppm. The two sharp signals are consistent with what would be expected for a chain structure for Te_4^{2-} with bridging and terminal tellurium atoms in a 1:1 ratio. Extraction of Na_2Te_4 should either confirm or deny this explanation and is currently under investigation. The ^{119}Sn NMR spectrum (Fig. 15) also indicated the presence of three signals, two broad resonances at -1090 ppm ($\Delta\nu_{\frac{1}{2}} \sim 800$ Hz) and -1170 ppm ($\Delta\nu_{\frac{1}{2}} \sim 700$ Hz) and a single sharp peak at -1217 ppm. No satellite structure was observed for any of these signals however the ^{119}Sn chemical shifts of -1170 and -1217 ppm correspond to those of $SnTe_3^{2-}$ and one of the previously observed, yet unidentified, signals.

In any event, this approach did not produce dinuclear tin species corresponding to that found in the lead system as obviously the tin is oxidized from the +2 to +4 oxidation state. Neither was any NMR evidence for the $Sn_2Te_6^{4-}$ species found.

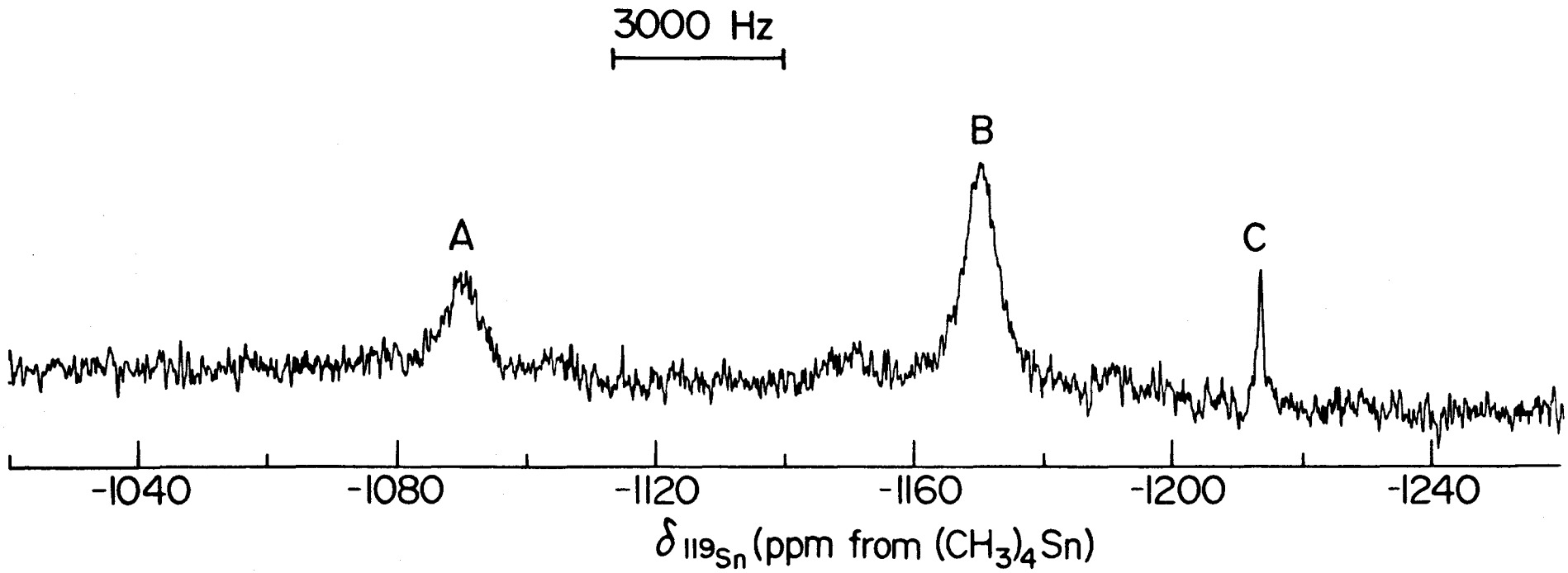

Fig. 15. ^{119}Sn NMR spectrum, obtained at 93.27 MHz, of the solution from the reaction of $SnCl_2$ and Te_2^{2-}: (A) and (C) are unassigned signals; (B) $SnTe_3^{2-}$.

CHAPTER VI

MÖSSBAUER STUDIES OF THE $SnCh_4^{4-}$ AND $Sn_2Se_6^{4-}$ ANIONS

INTRODUCTION

The multinuclear magnetic resonance approach to the study of the anions extracted from Zintl phases is undoubtedly the most comprehensive investigative technique available. The identity of many of the species present in solution can be established from the relative NMR satellite intensities, the observed coupling patterns (if any) and the number of signals present. However, as earlier studies in this laboratory indicated,[36] often more than one valence-bond structure can be written to represent a molecule which correlates with the observed NMR data. As was found with the $SnCh_3^{2-}$ series of anions,[36] determination of the formal oxidation state of the central tin atom can be all that is necessary to enable identification.

RESULTS AND DISCUSSION

Origin and Meaning of the Mössbauer Isomer Shift(δ) and Quadrupole Splitting (Δ).

Mössbauer spectroscopy is ideally suited to the study of the tin anions in the present work as ^{119}Sn is one

of the most studied nuclei by this technique. Mössbauer spectroscopy is concerned with the nuclear transitions that result from the resonant absorption of γ-rays by a sample. The electronic environment about the nucleus determines the energy necessary to cause the nuclear transitions which is characterized by different spin quantum numbers, I, for the ground and excited nuclear states. In the present study, Mössbauer parameters, the isomer shift (δ) and quadrupole splitting (Δ) for a given resonance, are sensitive to the electronic structure of the Mössbauer atom, ^{119}Sn, and the ligand environment about the tin atom. For tin Mössbauer spectroscopy, tin(II) and tin(IV) compounds normally give characteristic isomer shifts thereby providing the formal oxidation state of the tin atom in a molecule. Furthermore, any spectroscopic parameter which is sensitive to the electronic or molecular structure of a compound can be very useful in understanding the bonding in that compound. A brief presentation of the origin and meaning of the aforementioned Mössbauer parameters follows.

As stated above, the isomer shift and quadrupole splitting are the two most useful parameters obtained from a Mössbauer spectrum. Mössbauer spectroscopy is a resonant technique and as such any nucleus in a different chemical environment to that of the source nucleus will absorb the γ-energy at a different frequency from that of the source. It is this difference which is referred to as the Isomer

shift, δ. The isomer shift is usually described as in equation (16)

$$\text{Isomer Shift} = 2\kappa R^2 \frac{\delta R}{R} \{[\psi(0)_s]_a^2 - C\} \qquad (16)$$

where R = radius of the nucleus being studied, $|\psi(0)_s|_a$ is the s-electron density of the absorbing nucleus, κ is a nuclear constant, C is a source constant, and δR is the difference between the excited state and ground state radii of the observed nucleus. Given that δR is a constant for the nucleus in question, it is clear from equation (16) that the isomer shift is a direct measure of the overlap of the s-electron density with the nuclear charge density of the absorbing nucleus. The expression for the isomer shift was derived assuming the nucleus to be a uniformly charged sphere. However, if this assumption is relaxed, and if $I \geq \frac{1}{2}$ as for the excited state of tin, the interaction of the assymmetric electric fields about the nucleus with the nuclear charge density results in a splitting of the nuclear energy levels as shown in Fig. 16. The $I = \frac{1}{2}$ ground state remains degenerate while the I = 3/2 excited state level splits into two, and both of the possible transitions shown are allowed, the result being a two line spectrum. The magnitude of the quadrupole splitting is proportional to the Z-component of the electric field gradient (EFG) tensor which interacts with the quadrupole moment of the nucleus.

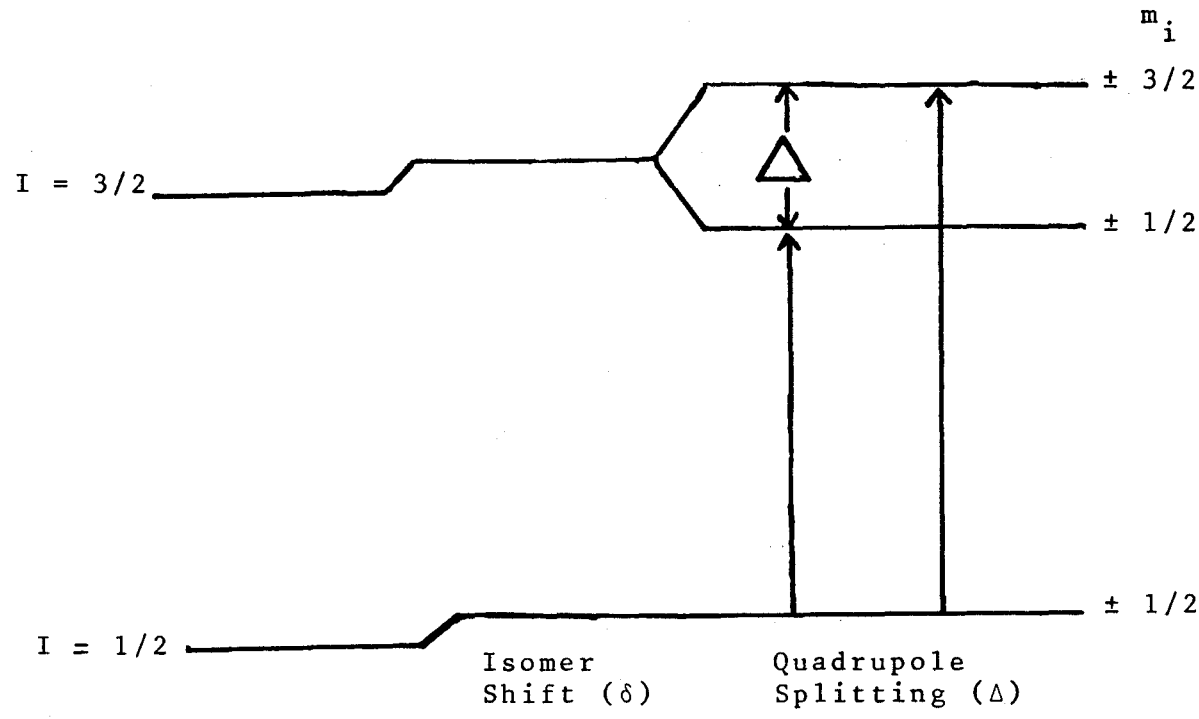

Fig. 16. Nuclear energy levels with the excited level (I = 3/2) split into two by the quadrupole interaction.

The parameters of the compounds studied in this work are given in Table 9. All isomer shift values are below a velocity of 2.65 mms^{-1} which is characteristic of tin in its +4 oxidation state.[52]

The $SnCh_4^{4-}$ Anions

Extraction of the NaSnTe and NaSnSe alloys with crypt in en gives solutions which contain the classically-bonded tetrahedral $SnTe_4^{4-}$ and $SnSe_4^{4-}$ anions. The structures of these two anions have been established by X-ray crystallo-

graphy,[28,29] with $SnSe_4^{4-}$ in $Na_4SnSe_4 \cdot 16H_2O$ and $SnTe_4^{4-}$ in Na_4SnTe_4, and both anions are reported to have a tetrahedral arrangement of selenium or tellurium atoms about the central tin atom. However, both anions have less than T_d symmetry in the solid state since all Sn-Ch bond lengths are not equal and the Ch-Sn-Ch angles are not 109.7° (the tetrahedral value), but vary from 102.9(4) to 115.0(4)°.[28,29] Table 9 contains the ^{119}Sn Mössbauer data for the two $SnCh_4^{4-}$ species. The isomer shifts for $SnSe_4^{4-}$ and $SnTe_4^{4-}$, 1.47 and 1.76 mms^{-1}, respectively, are very similar to those values ($\sim$1.5-1.8 mms^{-1}) found for the solids isolated from en solutions containing the $SnCh_3^{2-}$ series of anions[52] indicating similar bonding for these species (i.e. classical bonding). Since δR is positive for ^{119}Sn, an increase in the s-electron density at the absorber nucleus results in a more positive isomer shift. As expected, the isomer shift of $SnSe_4^{4-}$ is less positive than that of $SnTe_4^{4-}$ due to the greater electronegativity of selenium. Furthermore, the isomer shifts of both $SnSe_4^{4-}$ and $SnTe_4^{4-}$ are considerably smaller than those values ($\sim$2.2 - 3.0 mms^{-1}) found for the cluster Zintl anions[52] indicating that s-electron density has been removed from the tin atom in these species. The spectrum of $SnSe_4^{4-}$ is shown in Fig. 17 and consists of two lines of equal intensity with a quadrupole splitting of 0.62 mms^{-1}. The observation of a non-cubic environment about tin was not unexpected as, previously stated, in the solid state the anion has a symmetry lower than

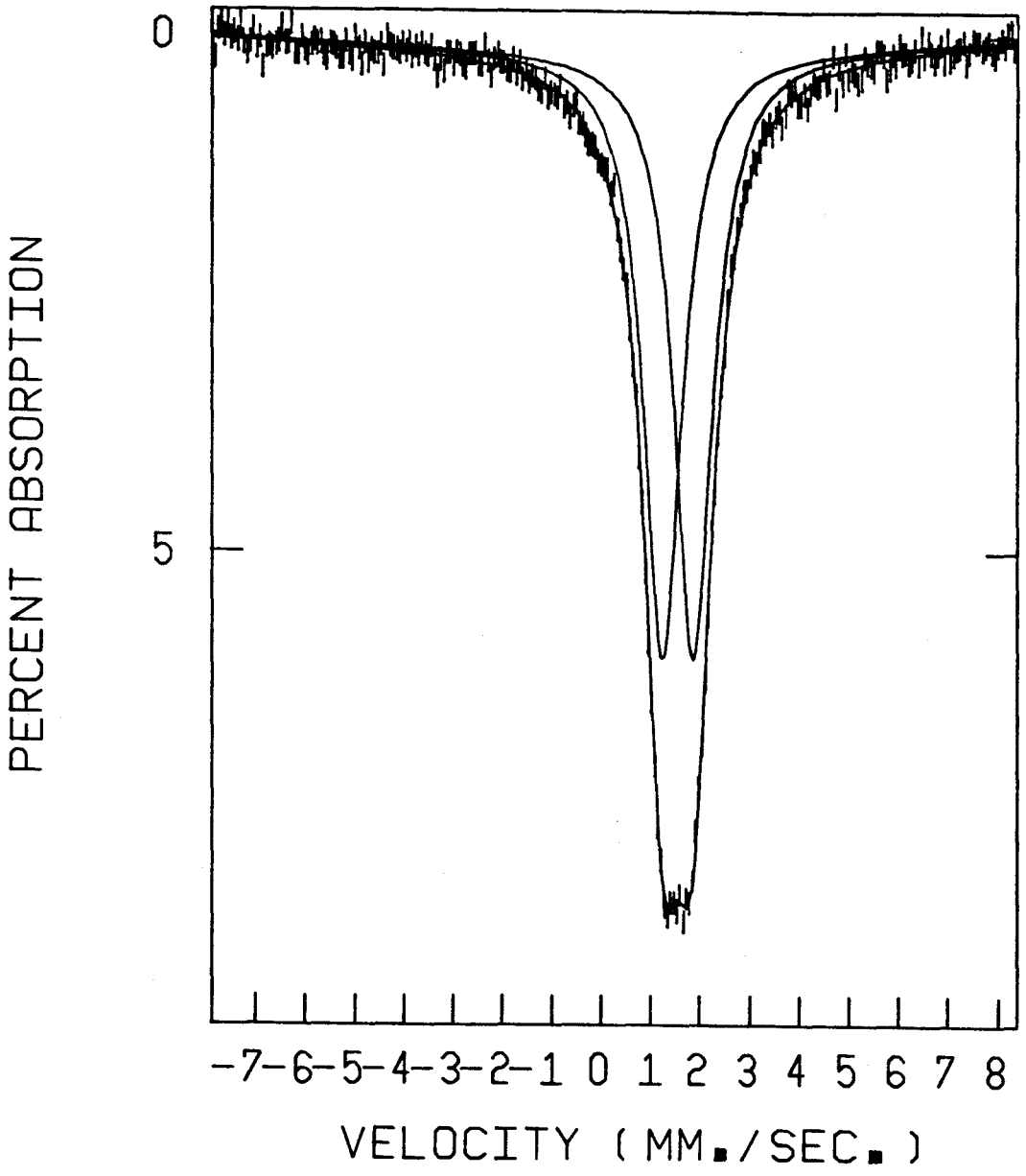

Fig. 17 ^{119}Mössbauer spectrum at 77K of $(Crypt\text{-}Na^{+})_4(SnSe_4)$.

T_d.[29] The $SnTe_4^{4-}$ resonance was also found to be a closely spaced quadrupole doublet with a splitting of 0.63 mms^{-1}. While the isomer shift of $SnTe_4^{4-}$ (1.76 mms^{-1}) is close to that reported for K_4SnTe_4 by Haushalter and co-workers (1.71(2) mms^{-1}),[49] only a single absorption for their compound was reported. Therefore, $SnSe_4^{4-}$ and $SnTe_4^{4-}$ must be distorted in the solid-state for the compounds studied in this work, as was found in the corresponding crystal structures. Frozen-solution spectra were also obtained however the spectra were not very good.

Mössbauer spectra of the solids isolated from the mixed selenium-tellurium alloy extractions were not obtained. In previous work[52] it was found that the parameters for the $SnTe_3^{2-}$ and $SnSe_3^{2-}$ anions did not vary by more than 0.2 mms^{-1}. The mixed species of the trigonal-planar $SnCh_3^{2-}$ series were always present in solution as a mixture of anions i.e. no intermediate species were produced independently. Thus detection of these anions individually by Mössbauer spectroscopy was not possible. Since the mixed anions of the tetrahedral series are also observed in solution as a mixture of anions, no Mössbauer investigation of the solids isolated from these solutions were undertaken.

The $(SnCh_3)_2^{2z-}$ Anions (z = 1 or 2)

Haushalter and co-workers[49] have reported the X-ray crystal structure of the $Sn_2Te_6^{4-}$ anion in $[(CH_3)_4N]_4Sn_2Te_6$

shown in structure (I) where the tin atoms are coordinated to four tellurium atoms in a pseudo-tetrahedral arrangement. The Mössbauer parameters for this compound are given in Table 9 and the observation of a quadrupole splitting reflects the non-cubic environments about the tin atoms. Interestingly, the isomer shift for this compound ($\sim$ 1.80 mms^{-1})[49] is very similar to that of the solid obtained from solutions of the $SnTe_3^{2-}$ anion, indicating the same s-electron density on tin. This might suggest that the $SnTe_3^{2-}$ anion does not maintain its trigonal-planar structure in the solid state. However, the quadrupole splitting (1.85 mms^{-1}) for the solid product isolated from solutions of $SnTe_3^{2-}$ is considerably larger than that of the $Sn_2Te_6^{4-}$ compound ($\sim$ 0.8 mms^{-1})[49] which implies that the salt in which the cation is cryptated contains a tin atom in a much more distorted environment than that found for $[(CH_3)_4N]_4[Sn_2Te_6]$. It was not known whether this difference in quadrupole splitting between $[(CH_3)_4N]_4Sn_2Te_6$ and $[Crypt\text{-}K^+]_{2z}[SnTe_3]_z$ resulted from the difference between a pseudo-tetrahedral and a trigonal-planar structure with $z = 1$. Unfortunately, as noted earlier, no evidence for the existence of the $Sn_2Te_6^{4-}$ anion in solution has been found so it was not possible to isolate a solid from such a solution in order to compare the Mössbauer parameters with those observed for the $[(CH_3)_4N][Sn_2Te_6]$ and $[Crypt\text{-}K^+]_{2z}[SnTe_3]_z$ compounds.

TABLE 9: ^{119}Sn Mössbauer Data for Classically-Bonded Zintl Anions[a]

Compound	Isomer Shift, δ (mms^{-1})	Quadrupole Splitting, Δ (mms^{-1})	Linewidth, Γ (mms^{-1})
$[Crypt\text{-}Na^+]_4[SnSe_4]$[b]	1.47	0.62	0.95
frozen soln[c]	1.43	0.95	1.38
$[Crypt\text{-}Na^+]_4[SnTe_4]$[b]	1.76	0.63	1.03
frozen soln[c]	1.61	0.97	1.35
$K_4[SnTe_4]$[d]	1.71(2)	-	-
$[Crypt\text{-}K^+]_2[SnTe_3]$	1.74	1.85	1.19
frozen soln	1.71	1.81	0.98
$[Crypt\text{-}K^+]_2[SnSe_3]$	1.51	1.19	0.96
frozen soln	1.53	1.80	1.15
$[Crypt\text{-}K^+]_4[Sn_2Se_6]$	1.55	1.17	0.89
frozen soln	1.52	1.23	0.87
$[(CH_3)_4N]_4[Sn_2Te_6]$[d]	$\sim$ 1.80	$\sim$ 0.80	-

[a] All spectra measured at 77 K. δ, Δ, and Γ values are ± 0.01 mms^{-1}.

[b] The first entry for each compound refers to the isolated solid, while the second entry refers to the frozen solution of the compound listed directly above.

[c] The frozen solution spectra were of poor quality as indicated by rather large linewidths associated with these spectra.

[d] Reference 49.

In the present work, solutions containing the $Sn_2Se_6^{4-}$ anion have been observed and the isolated solid, upon removal of the solvent, has been investigated by Mössbauer spectroscopy (Fig. 18). Table 9 contains the Mössbauer parameters for this anion and it is clear that while the isomer shift of this compound is similar to that of $[Crypt\text{-}K^+]_2[SnSe_3]_2$ so too is the quadrupole splitting. This suggests that the coordination of the tin atom in these two compounds is the same, therefore upon removal of the solvent from solutions containing $SnSe_3^{2-}$, the dimer, $Sn_2Se_6^{4-}$, is formed. To test this hypothesis further, frozen-solution Mössbauer spectra were obtained from solutions containing $SnSe_3^{2-}$ and $Sn_2Se_6^{4-}$. Again, the isomer shifts were virtually identical, but the quadrupole splittings differed substantially. More importantly, the quadrupole splittings for both the solid and frozen-solution samples of $Sn_2Se_6^{4-}$ were the same indicating identical coordination of the tin atoms in the solid state and solution. These values were considerably smaller than that found in the frozen-solution spectrum of $SnSe_3^{2-}$ (Fig. 19), which would be expected if $SnSe_3^{2-}$ exists as a dimer in the solid state with a pseudo-tetrahedral arrangement of selenium atoms about the tin atoms.

A frozen-solution Mössbauer spectrum of $SnTe_3^{2-}$ gave a similar isomer shift to that of the solid obtained from the same solution, but contrary to the $SnSe_3^{2-}$ case, the quadrupole splitting was the same in solution as it was in the solid. Evidently, removal of solvent from solutions of $SnTe_3^{2-}$ does not

result in the dimerization of this anion to $Sn_2Te_6^{4-}$. Therefore the very large difference in quadrupole splittings reported by Haushalter[49] for $[(CH_3)_4N]_4[Sn_2Te_6]$ and found in this work for $[Crypt\text{-}K^+]_2\ [SnTe_3]$ is most likely a reflection of the different bonding about tin in these compounds, distorted-tetrahedral and trigonal-planar, respectively.

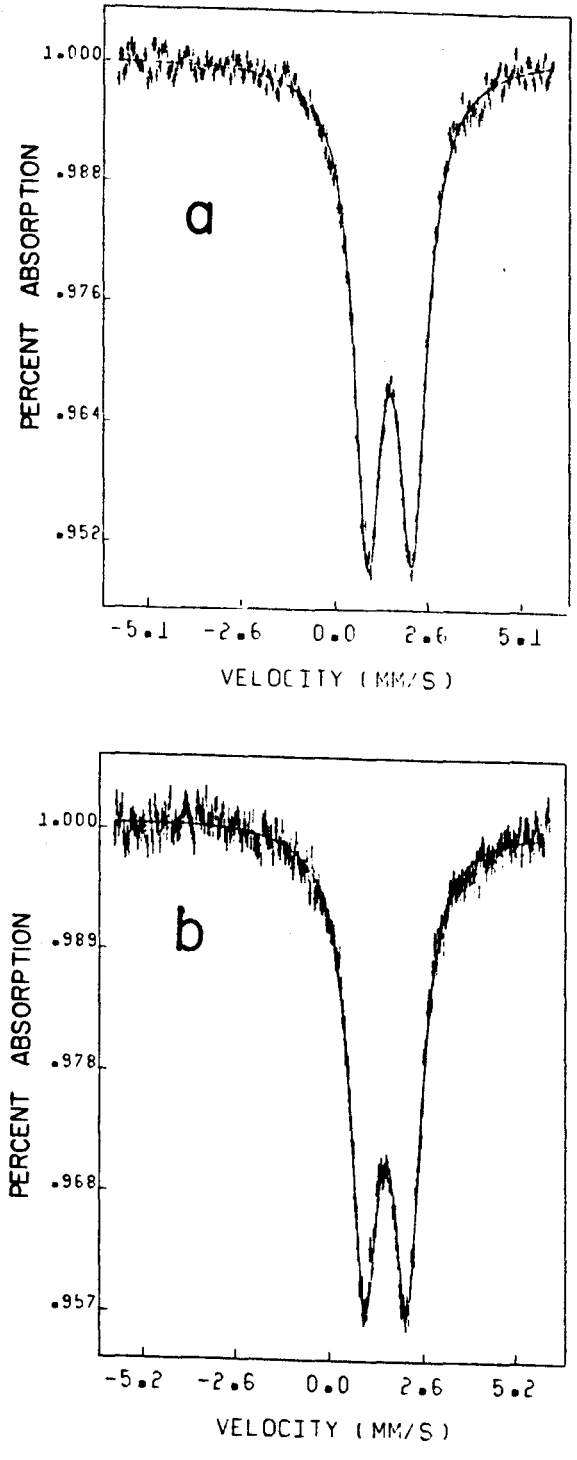

Fig. 18. ^{119}Sn Mössbauer spectra at 77K of $(Crypt\text{-}Na^{+})_4(Sn_2Se_6)$, (a) frozen solution and (b) solid.

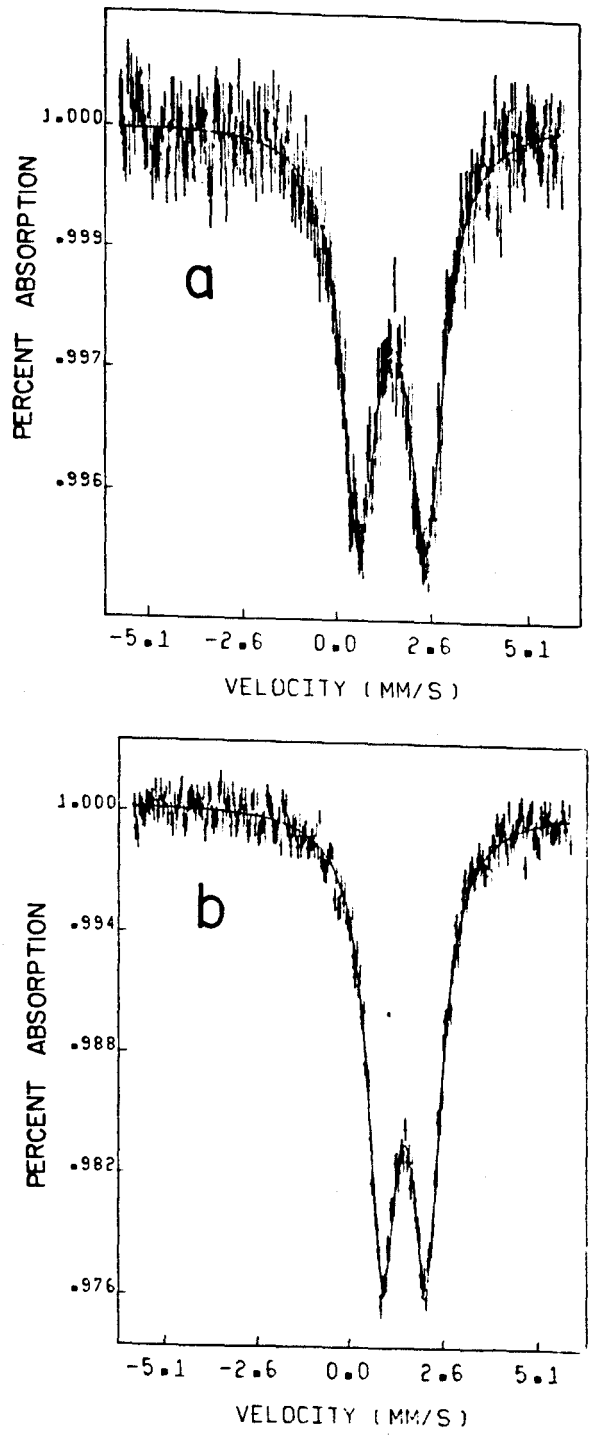

Fig. 19. ^{119}Sn Mössbauer spectra at 77K of $(Crypt\text{-}K^{+})_2(SnSe_3)$, (a) frozen solution and (b) solid.

CHAPTER VII

NMR AND X-RAY CRYSTALLOGRAPHIC STUDIES OF SOLUTIONS AND SOLIDS EXTRACTED FROM $NaTlTe_{2-x}Se_x$ (x=0, ½, 1, 3/2, 2) ALLOYS

INTRODUCTION

During this work classically-bonded tin anions have been observed in addition to the previously characterized classically-bonded $CdCh_2^{2-}$, $HgCh_2^{2-}$, $TlCh_3^{3-}$ and $SnCh_3^{2-}$ series of anions.[36] With the hopes of producing a four-coordinate thallium species a number of NaTlCh alloys were prepared and investigated by ^{205}Tl and ^{125}Te NMR spectroscopy. An X-ray crystallographic study of a single crystal obtained from the solution extracted from a $NaTlTe_2$ alloy was also performed.

RESULTS AND DISCUSSION

NMR Investigations

Initially an alloy of composition $NaTlTe_{1.5}Se_{0.5}$ was extracted with en and crypt over a two week period producing a characteristic reddish-brown solution as found with previous thallium alloy extracts.[36] Investigation of this solution by ^{205}Tl NMR spectroscopy revealed at least five groups of very

broad multiplets centered approximately at 2750, 2350, 1900, 1325 and 560 ppm (Fig. 20). The chemical shifts span the range observed for the $TlCh_3^{3-}$ series of anions (370-2800 ppm)[36] and are far removed from the resonances associated with the butterfly-shaped $Tl_2Ch_2^{2-}$ anions (7600 - 8100 ppm).[36] The appearance of these signals as multiplets would appear to indicate the presence of a species containing more than one thallium atom. Unfortunately for the present, no further information could be gathered on this system as thallium NMR capabilities no longer existed.* However, ^{125}Te NMR spectroscopy showed the presence of three signals at -65 (very broad, weak signal), -423 ($\Delta\nu_{\frac{1}{2}} \sim 825$ Hz) and +487 ppm ($\Delta\nu_{\frac{1}{2}} \sim 130$ Hz) and interestingly these signals showed no evidence of any $^{203,205}Tl$ coupling. However, the signal-to-noise ratios were very poor and these signals remain unassigned.

A small amount of crystalline material was observed in the NMR sample containing the $NaTlTe_{1.5}Se_{0.5}$ extracts and due to the complex nature of the ^{205}Tl NMR spectra, it was decided that the isolation of such crystals might prove to be more in-

---

* $^{203,205}Tl$ NMR frequencies (142.87 and 144.27 MHz, respectively. at 5.8719 Tesla) resonate outside the dynamic range of the Bruker WM-250 high-range probe, thus special procedures (outlined in Chapter II) must be taken in order to observe these nuclei. During this work, the hardware necessary for the thallium experiments was sold by Bruker Canada.

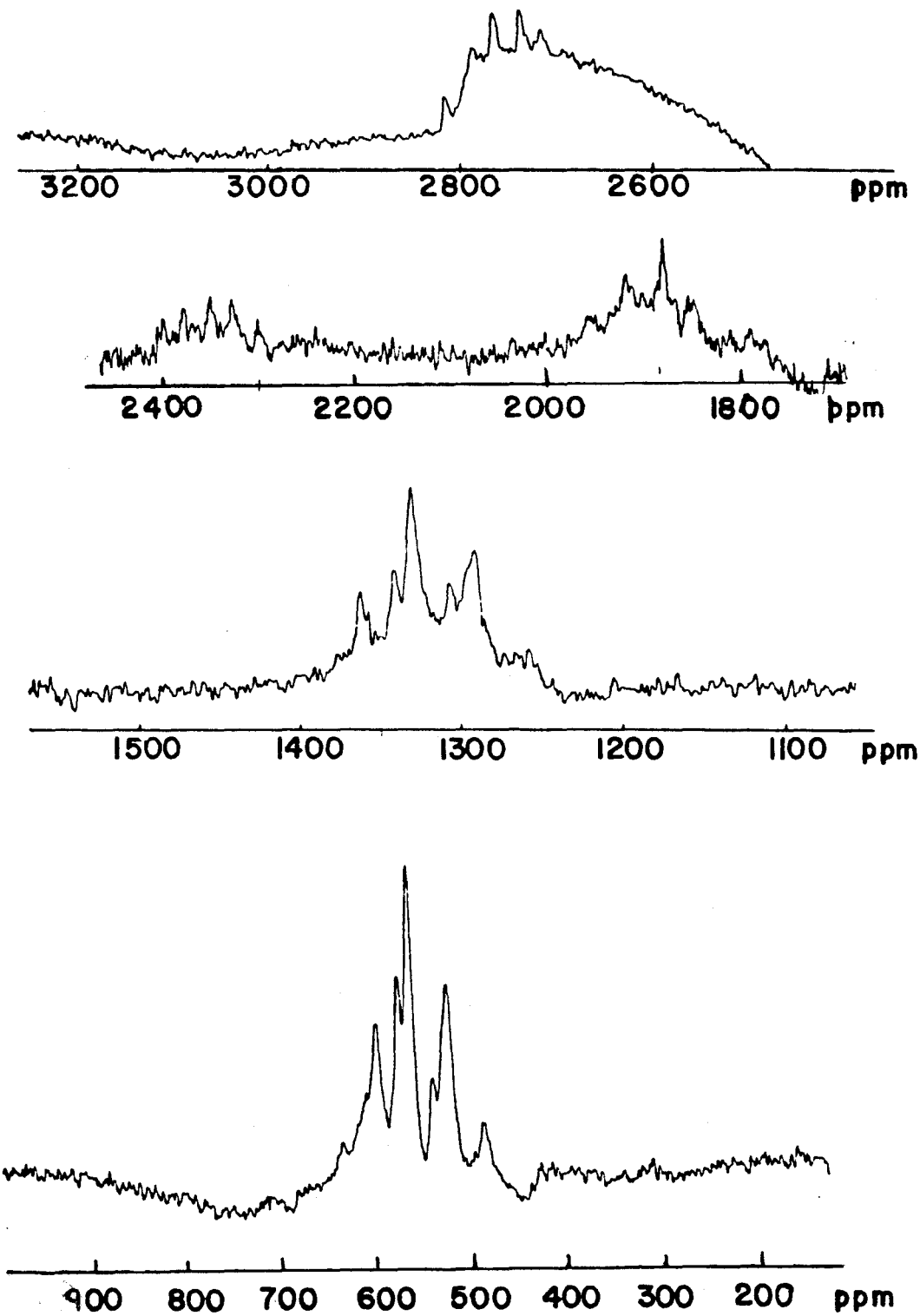

Fig. 20. ^{205}Tl NMR spectra obtained at 57.76 MHz, for the solution extracted from the $NaTlTe_{1.5}Se_{0.5}$ alloy.

formative. In this regard, a $NaTlTe_2$ alloy was prepared and extracted in the usual manner. A cherry-red colored solution was observed from which hexagonal-shaped violet-red crystals were grown. Several crystals were isolated, placed in 0.3 mm Lindemann capillaries, sealed and stored in a drybox. After two weeks the crystals had decomposed to a powder, probably due to a loss of en solvent. The experiment was repeated only this time the crystals were not as well formed as the previous set and did not diffract well at all. A crystal which did diffract was found, however, it turned out to be $(2,2,2\text{-crypt-}Na^+)_2Te_4^{2-}$ (see crystallographic section which follows).

A new NMR sample of the $NaTlTe_2$ alloy extract was prepared and investigated by ^{125}Te NMR spectroscopy in the hope of observing the as-of-yet unknown Te_4^{2-} anion in solution. A chemical shift range from -200 to +1060 ppm was explored but not a single resonance was observed. It must be noted here that the crystal studied was not one of the original chosen, nor did it bear any strong resemblance to any of the crystals grown earlier. This observation along with the lack of any evidence for the Te_4^{2-} anion in the ^{125}Te NMR spectrum casts serious doubt as to whether the crystal examined and found to be Te_4^{2-} is truly representative of this system. This sample was also tested for paramagnetism through both liquid and powder ESR spectroscopy but no evidence for such was observed. NMR samples of solutions extracted from $NaTlSe_2$, $NaTlTeSe$, $NaTlTe_{1.5}Se_{0.5}$ and $NaTlTe_2$ have been prepared and

await investigation by ^{205,203}Tl NMR spectroscopy when a new facility is in place.

Crystal Structure of [4,7,13,16,21-24-Hexaoxa-1, 10-Diazabicyclo[8·8·8]hexacosane sodium]Tetratelluride(2-), $(C_{18}H_{36}N_2O_6Na^+)_2Te_4^{2-}$.

Elements of Group VI form anionic chains of general formula Ch_x^{2-}. In the sulfur series S_3^{2-},[53] S_4^{2-},[54] S_5^{2-},[55,56] S_6^{2-},[57,58] and S_7^{2-},[59] have all been structurally characterized. The known structures of the polyselenides include Se_3^{2-},[60] Se_4^{2-},[61] Se_5^{2-},[62] and Se_6^{2-},[58] while the polytelluride series is represented by Te_3^{2-},[50] Te_4^{2-},[63] and Te_5^{2-},[64]. Although the stoichiometry and the characteristic deep red colored solutions of the Te_4^{2-} anion had been reported long ago,[65,5] it is only recently that the structure of this anion has been determined in $(Ph_4P^+)_2Te_4^{2-}\cdot 2CH_3OH$.[63] The present structure determination of Te_4^{2-} in $(2,2,2\text{-crypt-}Na^+)_2$-$Te_4^{2-}$, represents a Te_4^{2-} anion in an unsolvated environment with several differences in the gross structural features of this anion compared to the previously determined structure.

Some final atomic positional and thermal parameters are given in Table 10 while a view of the contents of the unit cell is shown in Fig. 21. The compound crystallizes in the monoclinic space group $\underline{P}2_1/\underline{c}$ with lattice constants $a = 10.710(5)$, $b = 12.038(9)$, and $c = 39.14(2)$ Å with $\beta = 95.07(4)°$ and $R_1 = 0.082$ and $R_W = 0.086$ for 2660 observed reflections.

TABLE 10: Some Final Atomic and Thermal Parameters[a] for $(2,2,2\text{-crypt-}Na^+)_2Te_4^{2-}$

Atom	x	y	z	U or U_{eq}
Te(1)	-908(2)	3621(2)	9127(1)	66.3 (15)
Te(2)	-100(2)	1563(2)	9152(1)	59.1 (13)
Te(3)	-954(2)	316(2)	8614(1)	59.4 (13)
Te(4)	676(2)	94(2)	8133(1)	68.4 (15)
Na(1)	6018(10)	2505(9)	427(3)	43(6)
Na(2)	3306(22)	5784(9)	2052(3)	45(6)

[a] $\underline{U}_{eq} = \frac{1}{3} \sum_i \sum_j a^*_i a^*_j \underline{a}_i \underline{a}_j \underline{U}_{ij}$

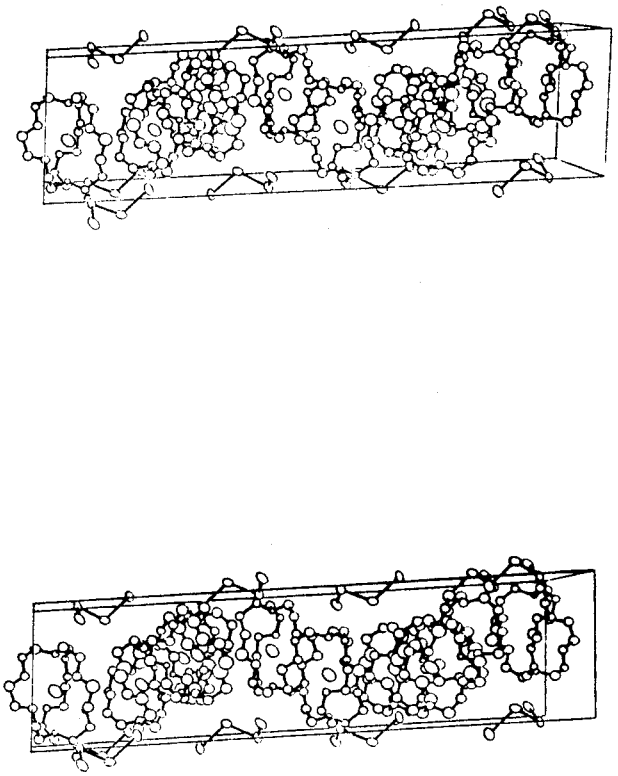

Fig. 21. ORTEP view of the crystal packing in $(2,2,2\text{-crypt-}Na^{+})_2Te_4^{2-}$.

Three-dimensional X-ray data were collected on an automated diffractometer using monochromated MoKα radiation at room temperature. The lattice contains cryptated sodium ions and tetratelluride anions, Te_4^{2-}, with the terminal bonds longer than the middle bond (Table 11). This shortening of the terminal bonds, relative to the internal bond, occurs in the previously characterized Te_4^{2-} anion[63] as well as the isostructural Se_4^{2-},[61] anion, however the reverse situation is found for the S_4^{2-} anion.[54] The Te-Te distances are 2.702(3) and 2.746(3)Å corresponding to the terminal and middle bonds, respectively. The Te-Te-Te bond angles are 109.7(1) and 110.0(1)° with a Te-Te-Te-Te dihedral angle of 105.3(1)°.

The Te-Te bond lengths in the present compound are significantly shorter than those in the tetraphenylphosphonium salt (2.724(1) x 2(end) and 2.762(1)Å (middle)).[63] Two other bonds to which Te_4^{2-} can be compared are those in Te_3^{2-} and Te_5^{2-}. The former has Te-Te bond lengths of 2.692(5) and 2.720(4)Å[50] which are somewhat shorter than observed for Te_4^{2-}. The pentatelluride anion in $(Bu_4N^+)_2Te_5^{2-}$,[64] has Te-Te bond lengths (2.704(1) x 2(end) and 2.746(1)Å x 2(middle)) comparable to Te_4^{2-} in $(2,2,2\text{-crypt-}Na^+)_2Te_4^{2-}$. In both $(Ph_4P^+)_2Te_4^{2-}\cdot 2CH_3OH$[63] and $(2,2,2\text{-crypt-}K^+)_2Te_3^{2-}\cdot en$[50], hydrogen bonding is considered to be responsible for some of the bond differences observed, however, such large lengthenings (0.02Å) in each case may not be due solely to solvation. The shortening of the terminal Te-Te bond lengths, 0.044Å, relative

to the middle Te-Te bond in the Te_4^{2-} anion in this work is similar to the terminal Te-Te bond shortenings found in the related Te_5^{2-} and solvated Te_4^{2-} anions. The dihedral angle in the tetraphenylphosphonium salt of 99.9(1)° is very much smaller than the present value of 105.3(1)° thus the present structure is a more open structure. Hordvik[65] noted there is a correlation between disulfide bond lengths and dihedral angles, presumably due to eclipsing of lone pairs on the chalcogen atoms involved. If this is so then as the dihedral angle decreases the lone pairs on the chalcogen atoms repel each other more effectively and this might account for the longer bond lengths found in the tetraphenylphosphonium salt. The geometries of the cryptated sodium cations were found to be comparable with those found in related salts such as $(2,2,2\text{-crypt-}Na^+)_3Sb_7^{3-}$,[18] and $(2,2,2\text{-crypt-}Na^+)_2Sn_5^{2-}$.[17] Additional structural parameters are contained in the full crystallographic study of this compound.[66]

The species Te_4^{2-} is isoelectronic with I_4^{2+} which has been deduced in solid $(AsF_6^-)_2I_4^{2+}$ and $(Sb_3F_{14}^-)(SbF_6^-)I_4^{2+}$ by Gillespie et al.,[67] and Birchall and Myers[68]. Interestingly, the I_4^{2+} cation has a rectangular structure and can be thought to consist of two I_2^+ cations held together by two weak bonds. This closed structure is completely different from the open-chain structure observed for Te_4^{2-}, while the isoelectronic species Te_3^{2-},[50] and I_3^{2+},[69] are also isostructural.

TABLE 11: Bond Lengths and Bond Angles in Some Catenated Compounds of Group VI Elements.

Ion	Bond Length[a] (A°)	Bond Angle[b] (deg.)	Compound	Str. Ref.
Te_4^{2-}	2.702(3),t	109.7(1)	$[2,2,2\text{-crypt-}Na^+)_2Te_4^{2-}$	this work
	2.746(3),m	110.0(1)		
		(105.3(1))		
Te_4^{2-}	2.724(1),t	110.78(4)	$(Ph_4P^+)_2(Te_4^{2-})\cdot 2CH_3OH$	63
	2.762(1),m	(99.85(12))		
Se_4^{2-}	2.325,t	110.7(1)	$(2,2,2\text{-crypt-}Ba^{2+})(Se_4^{2-})\cdot$en	61
	2.344,m	113.9(1)		
		(76.0(1))		
S_4^{2-}	2.074(1),t	109.76(2)	Na_2S_4	54
	2.061(1),m	(97.81(2))		
I_4^{2+},c	2.578(4)	91.67(6)	$(AsF_6^-)_2I_4^{2+}$	67
	2.264(4)	88.33(6)	$(Sb_3F_{14}^-)(SbF_6^-)I_4^{2+}$	
Te_3^{2-}	2.692(5)	113.1(2)	$(2,2,2\text{-crypt-}K^+)_2(Te_3^{2-})$	50
	2.720(4)			
Te_5^{2-}	2.704(1),t	107.2(1)	$(Bu_4N^+)_2Te_5^{2-}$	64
	2.746(1),m	105.1(1)		

a "t" denotes terminal (end) bond length, "m" denotes middle bond lengths.

b Angle in parentheses is dihedral angle.

c The quoted bond lengths and bond angles for I_4^{2+} represent an average value calculated from the three slightly different sets of data found in reference 67.

DIRECTIONS FOR FUTURE WORK

The present work has generated many more questions than it has answered and considerable work in this regard is still to be done. The following is a brief list of some of the possibilities for further research.

1). To produce the $Sn_2Te_6^{4-}$ anion in solution, perhaps using Haushalter's preparation.

2). To try to produce mixed dimeric species of general formula $Sn_2Ch_6^{4-}$ (Ch = Te and Se).

3). Investigate the formation of $Sn_2Se_6^{4-}$ in solution in greater detail, for example, a study of the ion-pair effects and subsequent equilibria associated with this system.

4). Grow and isolate cyrstals of the cryptated, as-of-yet, unidentified anions found during this work.

5). Prepare quaternary Na/Sn/Te/Se alloys with tin: chalcogen ratios of 3:2 and 4:3.

6). Investigation of the Na/Tl/Te/Se extracts by $^{203,205}Tl$ NMR spectroscopy and X-ray crystallography when possible.

REFERENCES

1. von Schnering, H. G. Angew. Chem. Int. Ed. Engl. 1981, 20, 33.
2. Krebs, B. Angew. Chem. Int. Ed. Engl. 1983, 22, 113.
3. Corbett, J. D. Prog. Inorg. Chem. 1976, 21, 129.
4. Johannis, A. Compt. Rend. Hebd. Acad. Sci. 1891, 113, 795; 1892, 114, 587.
5. Zintl, E.; Goubeau, J.; Dullenkopf, W. Z. Phys. Chem. Abt. A 1931, 154, 1.
6. Zintl, E.; Harder, A. Z. Phys. Chem. Abt. A 1931, 154, 47.
7. Zintl, E.; Dullenkopf, W. Z. Phys. Chem. Abt. B 1932, 16, 183.
8. Kummer, D.; Diehl, L. Angew. Chem. Int. Ed. Engl. 1970, 9, 895.
9. Diehl, L.; Khodadedeh, K.; Kummer, D.; Strähle, J. Z. Naturfrosch B 1976, 31, 522.
10. Diehl, L.; Khodadedeh, K.; Kummer, D.; Strähle, J. Chem. Ber. 1976, 109, 3404.
11. 4,7,13,16,21,24-hexaoxa-1,10,diazobicyclo[8.8.8]hexacosane, $N(C_2H_4OC_2H_4OC_2H_4)_3N$.
12. Lehn, J. M. Acc. Chem. Res. 1978, 11, 49.
13. Metz, B.; Moras, D.; Weiss, R. Chem. Comm. 1970, 217.
14. Belin, C. H. E.; Corbett, J. D.; Cisar, A. J. Am. Chem. Soc. 1977, 99, 7163.
15. Corbett, J. D.; Edwards, P. J. Am. Chem. Soc. 1977, 99. 3313.

16. Critchlow, S. C.; Corbett, J. D. J. Am. Chem. Soc. 1983, 105, 5715.

17. Edwards, P. A.; Corbett, J. D. Inorg. Chem. 1977, 16, 903.

18. Critchlow, S. C.; Corbett, J. D. Inorg. Chem. 1984, 23, 770.

19. Cisar, A.; Corbett, J. D. Inorg. Chem. 1977, 16, 2482.

20. Belin, C. H. E. J. Am. Chem. Soc. 1980, 102, 6036.

21. Adolphson, D. G.; Corbett, J. D.; Merrymann, D. J. J. Am. Chem. Soc. 1976, 98, 7234.

22. Wade, K. Adv. Inorg. Chem. Radiochem. 1976, 18, 1.

23. Rudolph, R. W. Acc. Chem. Res. 1976, 9, 446.

24. Corbett, J. D.; Critchlow, S. C.; Burns, R. C. "Rings, Clusters and Polymers of the Main Group Elements", ACS Symposium Series, Ed. A. H. Cowley. 1983, 232, 95.

25. Burns, R. C.; Corbett, J. D. J. Am. Chem. Soc. 1981, 103, 2627.

26. Burns, R. C.; Corbett, J. D. J. Am. Chem. Soc. 1982, 104, 2808.

27. Burns, R. C.; Corbett, J. D. Inorg. Chem. 1981, 20, 4433.

28. Eisenmann, B.; Schäfer, H.; Schrod, H. Z. Naturforsch. B, 1983, 38B, 921.

29. Krebs, V. B.; Hinter, H. Z. Anorg. Allg. Chem. 1980, 143, 462.

30. Critchlow, S. C.; Corbett, J. D. Inorg. Chem. 1982, 21, 3286.

31. Critchlow, S. C.; Corbett, J. D. Inorg. Chem. 1985, 24, in press.

32. Rudolph, R. W.; Wilson, W. L.; Taylor, R. C. J. Am. Chem. Soc. 1978, 100, 4629.

33. Rudolph, R. W.; Wilson, W. L.; Taylor, R. C. J. Am. Chem. Soc. 1981, 103, 2480.

34. Rudolph, R. W.; Taylor, R. C.; Young, D. C. "Fundamental Research in Homogeneous Catalysis", Plenum Press, New York, 1979, p. 997.

35. Teixidor, F.; Luetkens, M. L.; Rudolph, R. W. J. Am. Chem. Soc. 1983, 105, 149.

36. Burns, R. C.; Devereux, L. A.; Granger, P.; Schrobilgen, G. J. Inorg. Chem. 1985, 24, 2615.

37. Harris, R. K.; Mann, B. E. "NMR and the Periodic Table", Academic Press, New York, 1978.

38. Birchall, T.; Johnson, J. P. Can. J. Chem. 1979, 57, 160.

39. Bancroft, G. M.; Maddock, A. G.; Ong. W. K.; Prince, R. H.; Stone, A. J. J. Chem. Soc. A 1967, 1966.

40. Ramsey, N. F. Phys. Rev. 1953, 91, 303.

41. Reference 37, Ch. 3, p. 53.

42. Correlation coefficient is defined as
$R = (n\Sigma xy - \Sigma x\Sigma y)/[(n\Sigma x^2 - (\Sigma x^2 - (\Sigma x)^2)(n\Sigma y^2 - (\Sigma y)^2)]^{\frac{1}{2}}$,
where all symbols have their usual meanings.

43. Pople, J. A.; Santry, D. P. Mol. Phys. 1964, 8, 1.

44. Pyykkö, P. Adv. Quant. Chem. 1978, 11, 353.

45. Pyykkö, P.; Desclaux, J. P. Accts. Chem. Res. 1979, 12, 276.

46. Pyykkö, P.; Wiesenfeld, L. Mol. Phys. 1981, 43, 557.

47. Gillespie, R. J.; Granger, P.; Morgan, K. R.; Schrobilgen, G. J. Inorg. Chem. 1984, 23, 887.

48. Pyykkö, P. Chem. Phys. 1977, 22, 289.

49. Haushalter, J. C.; Haushalter, R. C.; Huffman, J. C.; Shenoy, G. K.; Umarji, A. M. Inorg. Chem. 1984, 23, 2312.

50. Corbett, J. D.; Cisar, A. Inorg. Chem. 1977, 16, 632.

51. Björgivinsson, M.; Schrobilgen, G. J. unpublished work, this laboratory.

52. Birchall, T.; Burns, R. C.; Devereux, L. A.; Schrobilgen, G. J. Inorg. Chem. 1985, 24, 890.

53. Goh, N. K. Dissertation, Munster 1974.

54. Tegman, R. Acta. Crystallogr. 1973, B29, 1463.

55. Bottcher, P.; Kruse, K. J. Less-Common Metals 1982, 83, 115.

56. Leclerc, B.; Kabre, I. Acta Crystallogr. 1975, B31, 1675.

57. Abrahams, S. C.; Grison, E. Acta Crystallogr. 1953, 6, 206.

58. Teller, R.; Krause, L.; Haushalter, R. Inorg. Chem. 1983, 22, 290.

59. Kanatzidis, M.; Baenziger, N.; Covcouvanis, D. Inorg. Chem. 1983, 22, 290.

60. von Schnering, H.; Goh, N. Naturwissenschaften 1974, 61, 272.

61. Konig, T.; Eisenmann, B.; Schäfer, H. Z. Naturforsch. 1982, 37B, 1245.

62. Bottcher, P. Z. Kristallogr. 1979, 150, 65.

63. Huffman, J. C.; Haushalter, R. C. Z. Anorg. Allg. Chem. 1984, 518, 203.

64. Teller, R. G.; Krause, L. J.; Haushalter, R. C. Inorg. Chem. 1983, 22, 1809.

65. Hordvik, A. Acta. Chem. Scand. 1966, 20, 1885.

66. Devereux, L. A.; Schrobilgen, G. J.; Sawyer, J. F. Acta Crystallogr. 1985, C, in press.

67. Gillespie, R. J.; Kapoor, R.; Faggiani, R.; Lock, C. J. L.; Murchie, M.; Passmore, J. J. Chem. Soc., Chem. Comm. 1983, 8.

68. Birchall, T.; Myers, R. D. J. Chem. Soc., Chem. Comm. 1982, 1174.

69. Merryman, D. J.; Corbett, J. D.; Edwards, P. Inorg. Chem. 1975, 14, 428.

APPENDIX A-1 ^{205}Tl Spectra of the $TlCh_3^{3-}$ Anions

Example: $TlTe_3^{3-}$ (77.3% ^{125}Te)

Isotopic Isomer	Multiplicity and Binominal Intensities	Statistical factor(s)	Probability % (p)	Abundance (s × p)
TeTeTe	1	1	$(.227)^3$	0.012
*TeTeTe	1:1	3	$(.773)(.227)^2$	0.119
*Te*TeTe	1:2:1	3	$(.773)^2(.227)$	0.407
*Te*Te*Te	1:3:3:1	1	$(.773)^3$	0.462

*Te denotes spin-active tellurium atom (^{125}Te)

Multiplicity Pattern for $TlTe_3^{3-}$

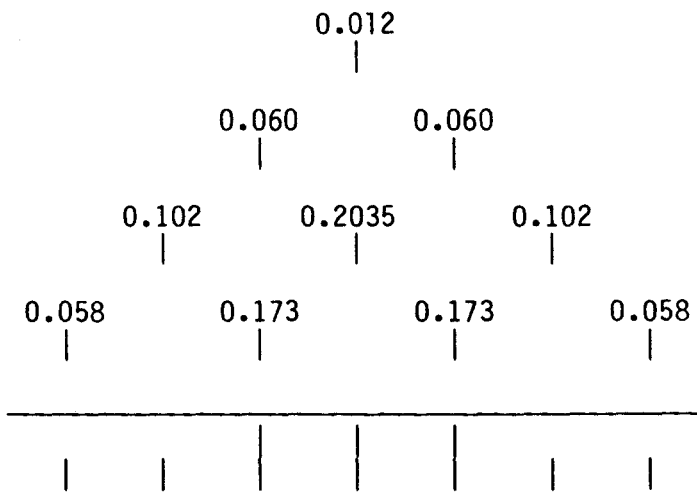

	0.058	0.102	0.233	0.215	0.233	0.102	0.058	Total Intensity Pattern
or	1	1.76	4.02	3.72	4.02	1.76	1	(relative intensities)

APPENDIX A-2: Method for Calculation of Satellite Intensities

The probability of obtaining an isotopomer of composition $^{1}A_{r}$, $^{2}A_{s}$,... $^{L}A_{q}$ for n chemically equivalent atoms of element A, in a molecule is given by formula (A1)

$$P_A = \frac{n!}{r!\ s!...q!} P_1^r P_2^s ....P_L^q \qquad (A1)$$

were P_i is the abundance of isotope i of (^{i}A) and q are the number of isotopes 1,2,....L; n = the number of chemically equivalent atoms A in a molecule and n = 2 + b + ...+ q.

The total probability, P_T, of each isotopomer for the molecule can then be obtained by forming the product of the chemically equivalent groups (A, B, C...,Q) in the molecule as shown in equation (A2)

$$P_T = P_A P_B P_C ... P_Q \qquad (A2)$$

The NMR spectrum for the molecule is then a superposition of the weighted average (by the probability-factor). The NMR spectrum of each isotopomer and can therefore, in principle, be calculated. In practice the environments which give rise to an NMR peak and which couple to other environments in the molecule can be observed and have to be considered. For example, the first order NMR spectrum which is coupled to n chemically equivalent atoms whose element contains one spin-½ NMR-active isotope of abundance P is a superposition of a singlet, doublet, triplet, etc.. The most intense lines of a singlet, triplet, quintet, etc. contribute to the central peak ("0 ") while the

most intense lines of a doublet, quartet, etc. contribute to the most intense satellite peaks ("1"). The intensity of the central peak and the satellite ("1") can therefore be calculated from formulas (A3) and (A4) and the corresponding ratio, "1"/"0", calculated.

$$\text{"0"} = \sum_{t=o}^{n} \frac{n!}{t!(n-t)!} (P/2)^t (1-P)^{n-t} \quad \frac{t!}{(t/2)!(t/2)!} \quad t \text{ even} \qquad \text{(A3)}$$

$$\text{"1"} = \sum_{t=1}^{n} \frac{n!}{t!(n-t)!} (P/2)^t (1-P)^{n-t} \quad \frac{t!}{(\frac{t}{2}-\frac{1}{2})!(\frac{t}{2}+\frac{1}{2})!} \quad t \text{ odd} \qquad \text{(A4)}$$

The number of elements each environment is bonded to can now be determined by comparing the measured ratio with the calculated one. In most cases the contribution of a quintet or higher spectrum is small due to their low probability. The ratio "1"/"0" can therefore be determined to a good approximation using formula (A5)

$$\frac{\text{"1"}}{\text{"0"}} = Xn \left[\frac{1 + (n-1)(n-2)X^2/2}{1 + n(n-1)X^2} \right] \qquad \text{(A5)}$$

$$X = \frac{P}{2(1-p)}$$

The relative satellite intensities for the $SnCh_3^{2-}$ series of anions are given in Table A-1.

TABLE A-1

Anion	Observed Nucleus	Satellite Nucleus	% Doublet Satellite Intensity (obs. (error), theor.)
$SnTe_3^{2-}$	^{119}Sn	^{125}Te	10.7±(0.7),11.3
	^{125}Te	^{119}Sn	4.7±(0.4),5.5
		^{117}Sn	4.7±(0.4),4.5
$SnTe_2Se^{2-}$	^{119}Sn	^{125}Te	7.6±(0.6),7.6
		^{77}Se	4.2±(0.6),4.1
	^{125}Te	^{119}Sn	4.7±(0.4),5.1
		^{117}Sn	4.5±(0.4),4.5
$SnTeSe_2^{2-}$	^{119}Sn	^{125}Te	3.7±(0.3),3.8
		^{77}Se	7.9±(0.3),8.2
	^{125}Te	^{119}Sn	4.8±(0.5),5.1
		^{117}Sn	4.2±(0.5),4.5
	^{77}Se	^{119}Sn	4.4±(0.8),5.1
		^{117}Sn	3.7±(0.8),4.5
$SnSe_3^{2-}$	^{119}Sn	^{77}Se	12.5±(0.7),12.2
	^{77}Se	^{119}Sn	4.8±(0.6),5.1
		^{117}Sn	4.1±(0.6),4.5

APPENDIX A-3 Satellite Intensities for the $SnCh_4^{4-}$ Anions

Anion	Observed Nucleus	Satellite Nucleus	% Doublet Satellite Intensity (obs. (error), theor.)
$SnTe_4^{4-}$	^{119}Sn	^{125}Te	14.8±(0.4),14.9
	^{125}Te	^{119}Sn	4.8±(0.6),5.1
		^{117}Sn	4.2±(0.6),4.5
$SnTe_3Se^{4-}$	^{119}Sn	^{125}Te	11.0±(0.7),11.4
		^{77}Se	4.0±(0.4),4.1
	^{125}Te	^{119}Sn	5.1±(0.4),5.1
		^{117}Sn	4.6±(0.4),4.5
$SnTe_2Se_2^{4-}$	^{119}Sn	^{125}Te	7.1±(0.7),7.6
		^{77}Se	7.8±(0.7),8.2
	^{125}Te	^{119}Sn	5.3±(0.4),5.1
		^{117}Sn	4.5±(0.4),4.5
	^{77}Se	^{119}Sn	4.8±(0.9),5.1
		^{117}Sn	4.5±(0.9),4.5
$SnTeSe_3^{4-}$	^{119}Sn	^{125}Te	3.7±(0.7),3.8
		^{77}Se	12.7±(0.7),12.3
	^{125}Te	^{119}Sn	5.5±(0.6),5.1
		^{117}Sn	4.4±(0.6),4.5
	^{77}Se	^{119}Sn	5.1±(0.4),5.1
		^{117}Sn	4.4±(0.4),4.5
$SnSe_4^{4-}$	^{119}Sn	^{77}Se	16.3±(0.4),16.1
	^{77}Se	^{119}Sn	5.2±(0.4),5.1
		^{117}Sn	4.2±(0.4),4.5